the polymerase chain reaction restriction fragment length polymorphism method according to a previous study.[7] Statistical significance was determined by the χ^2-test for differences of genotype and allele frequencies, and by the Student's *t*-test for differences of serum immunoglobulin (Ig)E levels and peripheral blood eosinophil counts among genotypes.

All studies were approved by the ethics review board of the Faculty of Medicine, University of Tokyo. All patients and controls involved gave their written informed consent for the genetic studies.

The frequencies of genotypes and alleles at the -1220 A/C SNP site are summarized in Tables 1 and 2. There was no significant difference in the genotype frequency between AD patients and controls ($P = 0.95$) or in the allele frequency ($P = 0.97$). Neither was there significant difference in the genotype frequency between PsV patients and controls ($P = 0.49$), nor in the allele frequency ($P = 0.39$). We estimated the statistical significance for a larger sample size (power calculation). If the sample size for both the patients and controls were increased 2630-fold (AD) or 5.15-fold (PsV), *P*-values would reach 0.05.

Table 1. Genotype frequencies of the -1220 A/C single nucleotide polymorphism of CYSLTR2 in AD patients, PsV patients and controls

Genotype	AD ($n = 158$)	Control ($n = 104$)	PsV ($n = 152$)
AA	138 (87.3)	91 (87.5)	139 (91.4)
AC	19 (12.0)	12 (11.5)	11 (7.2)
CC	1 (0.6)	1 (1.0)	2 (1.3)
	$P = 0.95$		$P = 0.49$

Comparisons of genotype distribution, using χ^2-test, showed no significant difference between AD patients and controls ($P = 0.95$) or between PsV patients and controls ($P = 0.49$). Numbers in parentheses indicate the percentage. AD, atopic dermatitis; CYSLTR2, CYSLT receptor 2; PsV, psoriasis vulgaris.

Table 2. Allele frequencies of the -1220 A/C single nucleotide polymorphism of CYSLTR2 in AD patients, PsV patients and controls

Allele	AD ($n = 158$)	Control ($n = 104$)	PsV ($n = 152$)
A	295 (93.4)	194 (93.3)	289 (95.1)
C	21 (6.6)	14 (6.7)	15 (4.9)
	$P = 0.97$		$P = 0.39$

Comparisons of allele distribution, using χ^2-test, showed no significant difference between AD patients and controls ($P = 0.97$) or PsV patients and controls ($P = 0.39$). Numbers in parentheses indicate the percentage. AD, atopic dermatitis; CYSLTR2, CYSLT receptor 2; PsV, psoriasis vulgaris.

Frequencies of the genotypes and alleles were not significantly different between AD with asthma and AD without asthma (data not shown). We compared the serum IgE levels and peripheral blood eosinophil counts among genotypes of AD patients, but no significant difference was observed (data not shown).

In this study, we demonstrated there was no association of the -1220 A/C CYSLTR2 SNP with AD or PsV. Previously, Fukai *et al.*[7] reported that the SNP was associated with asthma in a Japanese population. To the best of our knowledge, no association has been reported between PsV and any SNP of CYSLT or CYLTR.

The biological significance of CYSLT in AD has been suggested in some published work.[3,4] In addition, Hussain *et al.*[9] reported that a significantly higher number of CYSLTR1-positive cells were found in the dermis from an AD patient and in that from a psoriasis patient compared with those of normal skin. Montelukast is a leukotriene (LT) receptor antagonist that demonstrates high-affinity binding to the CYSLTR1, and in some randomized controlled trials, significant improvement of AD with montelukast treatment was found.[10] We evaluated -1220 A/C CYSLTR2 SNP to reveal the relation of CYSLTR2 with AD and PsV. Our result did not indicate the importance of the SNP in AD or PsV. However, because the sample size is small, any conclusion has to be interpreted with caution.

In summary, we showed that the -1220 A/C SNP of CYSLTR2 was not associated with AD or PsV in Japanese patients. This result suggests that this SNP is not a major player in the development of AD or PsV, at least in a Japanese population.

ACKNOWLEDGMENTS

This work was supported by Health Science Research Grants from the Ministry of Health Welfare and Labor of Japan and grants from the Ministry of Education, Culture Sports, Science and Technology of Japan.

Toyoaki KATO,[1] Hidehisa SAEKI,[1]
Yuichiro TSUNEMI,[1] Sayaka SHIBATA,[1]
Takashi SEKIYA,[2] Koichiro NAKAMURA,[3]
Takashi KAKINUMA,[1] Shinji KAGAMI,[1]
Hideki FUJITA,[1] Yayoi TADA,[1]
Makoto SUGAYA,[1] Kunihiko TAMAKI[1]

Departments of [1]Dermatology and [2]Allergy and Rheumatology, Faculty of Medicine, University of Tokyo, Tokyo, and [3]Department of Dermatology, Saitama Medical University, Saitama, Japan

REFERENCES

1 Samuelsson B. Leukotrienes: mediators of immediate hypersensitivity reactions and inflammation. *Science* (New York, NY) 1983; **220**: 568–575.
2 Lynch KR, O'Neill GP, Liu Q *et al.* Characterization of the human cysteinyl leukotriene CysLT1 receptor. *Nature* 1999; **399**: 789–793.
3 Sansom JE, Taylor GW, Dollery CT, Archer CB. Urinary leukotriene E4 levels in patients with atopic dermatitis. *Br J Dermatol* 1997; **136**: 790–791.
4 James JM, Kagey-Sobotka A, Sampson HA. Patients with severe atopic dermatitis have activated circulating basophils. *J Allergy Clin Immunol* 1993; **91**: 1155–1162.
5 Pillai SG, Cousens DJ, Barnes AA *et al.* A coding polymorphism in the CYSLT2 receptor with reduced affinity to LTD4 is associated with asthma. *Pharmacogenetics* 2004; **14**: 627–633.
6 Thompson MD, Storm van's Gravesande K, Galczenski H *et al.* A cysteinyl leukotriene 2 receptor variant is associated with atopy in the population of Tristan da Cunha. *Pharmacogenetics* 2003; **13**: 641–649.
7 Fukai H, Ogasawara Y, Migita O *et al.* Association between a polymorphism in cysteinyl leukotriene receptor 2 on chromosome 13q14 and atopic asthma. *Pharmacogenetics* 2004; **14**: 683–690.
8 Fauler J, Neumann C, Tsikas D, Frolich J. Enhanced synthesis of cysteinyl leukotrienes in psoriasis. *J Invest Dermatol* 1992; **99**: 8–11.
9 Hussain I, Kitagaki K, Businga TR, Kline JN. Expression of cysteinyl leukotriene receptor-1 in skin. *J Am Acad Dermatol* 2004; **51**: 1032–1033.
10 Yanase DJ, David-Bajar K. The leukotriene antagonist montelukast as a therapeutic agent for atopic dermatitis. *J Am Acad Dermatol* 2001; **44**: 89–93.

Normal human epidermal keratinocytes react differently than HaCaT keratinocyte cell line on exposure to *Propionibacterium acnes*

Dear Editor,

Keratinocytes play some role in the skin innate immunity and express keratinocyte differentiation-inducing proteins on exposure to *Propionibacterium acnes*.[1] Because normal human epidermal keratinocyte (NHEK) is not an immortalized cell *in vitro* and its culture treatment is complex, the spontaneously immortalized human keratinocyte cell line, HaCaT, is often used as a substitute for NHEK in *in vitro* studies of keratinocytes because of its ease in handling. This study compared the reactivity of NHEK and HaCaT on exposure to *P. acnes* and clarified whether substituting HaCaT for NHEK is appropriate.

Four strains of NHEK isolated from neonatal foreskin and from adult skin obtained from Cascade Biologics (Portland, OR, USA) and Cell Applications (San Diego, CA, USA) were grown using 154S medium (Cascade) supplemented with HKGS supplement (Cascade) at 37°C in an atmosphere of 5% (v/v) CO_2 in air. HaCaT were grown using Dulbecco's modified Eagle's medium (Invitrogen, Carlsbad, CA, USA) supplemented with 10% fetal bovine serum under the same conditions as NHEK. *P. acnes* JCM 6425 and JCM 6473 were maintained by harvesting in phosphate-buffered saline (pH 7.0) following culturing on modified GAM agar medium (Nissui Pharmaceutical, Tokyo, Japan) at 37°C under anaerobic conditions for 48 h. After 1×10^6 keratinocytes and 3×10^8 *P. acnes* were co-cultured for 1, 3, 6 or 24 h at 37°C in an atmosphere of 5% (v/v) CO_2 in air, mRNA were isolated from keratinocytes using Trizol reagent (Invitrogen). The relative abundance of mRNA of inflammatory cytokines (interleukin [IL]-1α, IL-6 and IL-8), keratinocyte differentiation-inducing proteins

Correspondence: Narifumi Akaza, Department of Dermatology, Fujita Health University School of Medicine, 1-98 Dengakugakubo, Kutsukake-cho, Toyoake, Aichi 470-1192, Japan. Email: akaza.narifumi@menard.co.jp

Journal of Dermatological Science 62 (2011) 42–49

Contents lists available at ScienceDirect

Journal of Dermatological Science

journal homepage: www.elsevier.com/jds

An environmental contaminant, benzo(a)pyrene, induces oxidative stress-mediated interleukin-8 production in human keratinocytes via the aryl hydrocarbon receptor signaling pathway

Gaku Tsuji [a,*], Masakazu Takahara [a], Hiroshi Uchi [a,b], Satoshi Takeuchi [a], Chikage Mitoma [a,b], Yoichi Moroi [a], Masutaka Furue [a,b]

[a] Department of Dermatology, Graduate School of Medical Sciences, Kyushu University, Fukuoka, Japan
[b] Research and Clinical Center for Yusho and Dioxin, Kyushu University Hospital, Fukuoka, Japan

ARTICLE INFO

Article history:
Received 18 May 2010
Received in revised form 30 September 2010
Accepted 3 October 2010

Keywords:
AhR
ROS
IL-8
Inflammation

ABSTRACT

Background: Benzo(a)pyrene (BaP) is an environmental contaminant found in cigarette smoke. It is well known that cigarette smoking exacerbates interleukin-8 (IL-8)-related inflammatory skin diseases such as psoriasis, palmoplantar pustulosis and acne. Although BaP has been shown to exert its biological effects via the aryl hydrocarbon receptor (AhR) signaling pathway, the mechanism of its inflammatory effects on skin remains unanswered.
Objective: To elucidate whether or not BaP cause AhR activation and subsequent oxidative stress leading to IL-8 production in normal human epidermal keratinocytes (NHEKs).
Methods: NHEKs exposed to BaP were analyzed. Immunofluorescence, real-time PCR, Western blotting, ELISA, reactive oxygen species (ROS) detection using H2DCFDA and RNA interference using si (small interfering) RNA were employed.
Results: Immunofluorescence analysis clearly demonstrated that BaP induced nuclear translocation of AhR from cytoplasm. The AhR activation subsequently induced CYP1A1 mRNA and protein expression in a dose-dependent manner. In addition, ROS and IL-8 production were coordinately augmented by BaP, whereas this was not the case in IL-1α, IL-6, TNF-α or GM-CSF production. Knockdown of AhR expression using siRNA transfection inhibited BaP-induced-ROS and IL-8 production, suggesting that these responses are strongly dependent on the AhR signaling pathway. Furthermore, the addition of N-acetyl cystein or catalase cancelled the IL-8 production by BaP, indicating that ROS production is essential for IL-8 production.
Results: This data highlights AhR-ROS-dependent regulation of IL-8 in NHEKs by BaP, providing a plausible explanation, at least in part, for why cigarette smoking exacerbates IL-8-related skin diseases such as psoriasis, palmoplantar pustulosis and acne.

1. Introduction

Health hazards posed by environmental contaminants have been brought to the public's attention and the results of numerous studies have been published. The skin functions as an immune organ against outside chemicals and pathogens. Several studies have been conducted on carcinogenesis by environmental contaminants [1,2]; however, little is known about the mechanism of inflammatory reactions to environmental contaminants in the skin [3]. Benzo(a)pyrene (BaP) is an environmental contaminant found in tabacco smoke and one of polycyclic aromatic hydrocarbons (PAHs). Studies on the carcinogenic potential of PAHs have revealed that they are metabolized through aryl hydrocarbon receptor (AhR) signaling pathways in internal organs such as the liver, lung, and colon [4–6]. However, there are few studies on the metabolism and biology of PAHs in the skin.

In general, the metabolism of PAHs via AhR signaling pathways occurs as follows [7]: (1) Upon cellular entry, PAHs interact with AhR located in the cytoplasm. (2) The PAHs-AhR complex subsequently translocates to the nucleus and forms the heterodimer PAHs/AhR/AhR nuclear translocator (ARNT) in the nucleus. (3) This PAHs/AhR/ARNT complex binds to specific xenobiotic responsive elements (XREs) to synthesize cytochrome P450 enzymes family including subfamily A, polypeptide 1 (CYP1A1). CYP1A1, also known as aryl hydrocarbon hydroxylase, is involved

* Corresponding author. Tel.: +81 92 642 5585; fax: +81 92 642 5600.
E-mail address: gakku@dermatol.med.kyushu-u.ac.jp (G. Tsuji).

0923-1811/$36.00 © 2011 Japanese Society for Investigative Dermatology. Published by Elsevier Ireland Ltd. All rights reserved.
doi:10.1016/j.jdermsci.2010.10.017

in the metabolization and activation of PAHs to produce reactive oxygen species (ROS). The main cause of carcinogenesis induced by PAHs is oxidative DNA damage exposed to ROS [6]. Furthermore, ROS plays a pivotal role in the intracellular signals and is capable of regulating the expression of proinflammatory cyto/chemokines [8].

Considering that BaP is present in tabacco smoke and in the surrounding environment, and that smoking is an aggravating factor in inflammatory skin diseases such as psoriasis [9–12], acne [13], and palmoplantar pustulosis [14–16], which are associated with neutrophil infiltration, we hypothesized that BaP might be capable of inducing interleukin (IL)-8 (a potent neutrophil chemoattractant) and other proinflammatory cyto/chemokines from normal human epidermal keratinocytes (NHEKs). The aim of the present study was to clarify whether or not BaP was able to activate AhR signaling pathways in NHEKs leading to ROS and proinflammatory cyto/chemokines production, which, to our knowledge, was previously unreported.

2. Materials and methods

2.1. Materials

Benzo(a)pyrene (BaP), N-acetyl cysteine (NAC), catalase and dimethyl sulfoxide (DMSO) were purchased from Sigma Chemical Co. (St. Louis, MO, USA). Anti-AhR rabbit IgG antibody (H-211), anti-CYP1A1 mouse IgG antibody (B-2), anti-GAPDH rabbit IgG antibody (FL-335), normal rabbit IgG, and normal mouse IgG were products of Santa Cruz Biotechnology (Santa Cruz, CA, USA).

2.2. Cell culture

NHEKs were obtained as cryopreserved first-passage cells from Clonetics-BioWhittaker (San Diego, CA, USA). They were grown in 100-mm tissue culture dishes in serum-free keratinocyte growth medium KGM-2 (Lonza, Walkersville, MD, USA) supplemented with bovine pituitary extract, human recombinant epidermal growth factor, insulin, hydrocortisone, transferrin, and epinephrine at 37 °C, 5% CO_2. The media was replaced daily. When near confluence (70–90%), cells were disaggregated with 0.25% trypsin/0.01% ethylenediamine tetraacetic acid (EDTA) in HEPES and subcultured. All experimental procedures were performed using second- to fourth-passage cells.

2.3. BaP exposure

On the day of the experiment, various concentrations (20 nM, 40 nM, 100 nM, 1 μM and 10 μM) of BaP were prepared in cell culture medium. Control cultures received medium containing a comparable DMSO concentration (up to 0.05%). Fresh medium containing either the appropriate BaP dose or DMSO was added. Cell counting was conducted using a hemocytometer, and viability was determined using trypan blue dye exclusion.

2.4. Immunofluorescence and confocal laser scanning microscopic analysis

NHEKs on glass tissue culture chamber slides were washed for 5 min × 3 times in phosphate-buffered saline (PBS), fixed with cold acetone for 10 min, and blocked using 10% bovine serum albumin (BSA) in PBS for 30 min at room temperature. Samples were incubated with primary rabbit anti-AhR (1:50) in PBS overnight at 4 °C. Slides were washed in PBS for 5 min × 3 times prior to incubation with anti-rabbit (Alexa Fluor 546, Molecular Probes, Eugene, OR, USA) secondary antibody for 1.5 h at room temperature in the dark. Slides were washed in PBS for 5 min × 3 times and mounted with ProLong Gold antifade reagent with DAPI (Invitrogen, Carlsbad, CA, USA). All samples were analyzed using a Nikon D-Eclipse confocal laser scanning microscope (Nikon, Tokyo, Japan).

2.5. Reverse transcription-polymerase chain reaction (RT-PCR) and quantitative real-time PCR (qRT-PCR) analysis

Total RNA was extracted using a commercially available kit (RNeasy Mini Kit; Qiagen, Valencia, CA, USA). Reverse transcription was performed using the PrimeScript™ RT-PCR Kit (Takara Bio, Shiga, Japan). PCR was performed in the following manner: 1 cycle of denaturation at 95 °C for 10 s, 30 cycles of denaturation at 90 °C for 5 s, extension at 60 °C for 20 s. The PCR products were analyzed using electrophoresis and densitometric analysis was performed using ImageJ software. ImageJ is a public domain, Java-based image processing program developed at the National Institutes of Health (New York, NY, USA). Quantitative RT-PCR was performed on the Mx3000p real-time system (Stratagene, La Jolla, CA, USA) using SYBR® Premix Ex Taq™ (Takara Bio). Amplification was started at 95 °C for 10 s as the first step, followed by 35 successive cycles of PCR: at 95 °C for 5 s, at 60 °C for 20 s. PCR data were exported to Excel (Microsoft, Redmond, WA, USA) for further analysis. Expression of CYP1A1 was measured in triplicate and was normalized for GAPDH expression levels. Primers, purchased from Takara Bio and SABiosciences (Frederick, MD, USA), were as follows:

AhR: forward 5′-ATCACCTACGCCAGTCGCAAG -3′ and reverse: 5′-AGGCTAGCCAAACGGTCCAAC-3′

GAPDH: forward 5′-GCACCGTCAAGGCTGAGAAC -3′ and reverse: 5′-TGGTGAAGACGCCAGTGGA -3′.

The sequence of CYP1A1 is not open. We used PPH01271E (SABiosciences).

2.6. Western blotting analysis

NHEKs were washed twice with PBS and then incubated in lysis buffer (50 mM HEPES, pH 7.4, 1% Triton X-100, 0.1% SDS, 150 mM NaCl, 1 mM EDTA, 20 μg/ml phenylmethylsulfonyl fluoride, 1 μg/ml leupeptin, 1 μg/ml pepstatin A, and 2 μg/ml aprotinin) for 5 min. The protein concentration of the lysate was measured using the BCA Protein Assay Kit (Pierce, Rockford, IL, USA). Equal amounts of protein (10 μg) were dissolved in NuPage LDS Sample Buffer (Invitrogen) and 10% NuPage Sample Reducing Agent (Invitrogen). The lysates were boiled at 70 °C for 10 min and then loaded and run on 4–12% NuPage Bis–Tris Gels (Invitrogen) at 200 V for 40 min. The proteins were then transferred onto PVDF membranes (Invitrogen) and blocked in 2% BSA in 0.1% Tween-20 (Sigma–Aldrich) and tris-buffered saline. The membranes were then probed with anti-AhR or anti-CYP1A1 antibodies overnight at 4 °C. Anti-rabbit or anti-mouse horseradish peroxidase-conjugated IgG antibody was used as a secondary antibody. Detection of protein bands was carried out using the Western Breeze Kit (Invitrogen) and visualization by autoradiography. Densitometric analysis of antibody responses on Western blotting was performed using ImageJ software (National Institutes of Health).

2.7. Detection of intracellular ROS production

2′,7′-dichlorofluorescein diacetate (DCFH-DA; Molecular Probes, Eugene, OR, U.S.A.) is a cell-permeable non-fluorescent probe that is de-esterified intracellularly and rapidly oxidized to highly fluorescent 2′,7′-dichlorofluorescein (DCF) in the presence of ROS (especially hydrogen peroxide). For the assays, quiescent confluent monolayer cultures on glass chamber slides were

preincubated with DCFH-DA (5 μM) solubilized in DMSO for 30 min at 37 °C, washed three times with PBS, and the fluorescence signal of DCFH (Ex = 490 nm; Em = 510 nm), the oxidation product of DCFH-DA, was analyzed on the stage of a using a Nikon D-Eclipse confocal laser scanning microscope. Then intracellular ROS production was visualized by the software EZ-C1 (Nikon) and fluorescence signal intensities were compared.

2.8. Enzyme-linked immunosorbent assay (ELISA)

The Multi-Analyte Profiler ELISArray Kit (SABiosciences) and IL-8 ELISA Kit (Invitrogen) were used to develop IL-1α, IL-6, IL-8, TNF-α and GM-CSF, according to the manufacturers' protocol. Optical density was measured using a Labsystems Multiskan MS Analyser (Thermo Bio-Analysis Japan, Tokyo, Japan).

2.9. Transfection with AhR or CYP1A1-targeted specific si (small interference) RNA

SiRNA targeted against AhR (si-AhR(1), s1199), (si-AhR, s1200), CYP1A1 (si-CYP(1), s3801), (si-CYP(2), s3802) and siRNA consisting of a scrambled sequence that would not lead to specific degradation of any cellular message (si-control) were purchased from Ambion (Austin, TX, USA). NHEKs cultured in 24-well plates, were incubated with the mix from the HiPerFect Transfection Kit (Qiagen, Courtaboeuf, France) containing 10 nM siRNA and 3.0 μl of HiPerFect reagent in 0.5 ml of culture medium, according to the manufacturer's instructions. After a 48 h incubation period, siRNA-transfected-NHEKs were exposed to BaP for an additional 24 h. SiRNA transfection did not affect cell viability, as demonstrated by light microscopic examination of the cultures (data not shown).

2.10. Statistical analysis

The unpaired student's *t*-test was used to analyze the results, and a *p*-value of less than 0.05 was considered to be statistically significant.

3. Results

3.1. Cell viability

After exposure to BaP (20 Nm–10 μM) for 24 h, NHEKs were examined under phase-contrast microscopy and their viabilities were determined using trypan blue dye exclusion methods. BaP did not affect the cell viability nor the morphological features of NHEKs (data not shown).

3.2. Nuclear translocation of AhR from cytoplasm was induced by BaP exposure

Since activation of AhR signaling pathways requires the nuclear translocation of AhR from cytoplasm, we first examined whether or not BaP was able to induce nuclear translocation of AhR in NHEKs. NHEKs grown on coverslips were treated with DMSO (control), or 1 μM BaP for 3 h and 6 h. The intracellular distribution of AhR was observed by immunofluorescence confocal laser scanning microscopy. Under normal conditions (DMSO-treatment), AhR was located in the cytoplasm of NHEKs (Fig. 1a). AhR started to appear in the nucleus as early as 3 h following BaP addition (Fig. 1b). Consequently, AhR staining was observed mostly in the nucleus at 6 h, confirming that BaP administration induced the nuclear translocation of AhR from cytoplasm in NHEKs (Fig. 1c). Fig. 1 (d) showed staining with rabbit iso-type IgG, which is the negative control.

3.3. BaP induced CYP1A1 mRNA and protein expression in NHEKs

We next examined whether or not the engagement of BaP to AhR induced expression of CYP1A1, a metabolizing and activating enzyme for BaP. NHEKs were exposed to either DMSO (control) or various concentrations of BaP (20 nM, 40 nM, 100 nM, 1 μM and 10 μM) for 3 h, 6 h and 24 h. The mRNA levels of CYP1A1 were measured by qRT-PCR. The mRNA levels of CYP1A1 were up-regulated in a dose-dependent manner at 3 h following BaP exposure (Fig. 2a). Furthermore, Western blotting analysis revealed that protein levels of CYP1A1 were up-regulated by BaP in a dose-dependent manner (Fig. 2b).

3.4. BaP induced ROS production in a dose-dependent manner

As several studies have demonstrated the production of ROS in the metabolizing process of BaP by CYP1A1 [4,5], we next examined whether or not BaP exposure was able to induce ROS production in NHEKs via the AhR signaling pathway. Compared to DMSO-treatment (control) (Fig. 3a), intracellular ROS was readily detectable in NHEKs by DCFH-DA fluorescence assay in a dose-dependent manner after addition of BaP 100 nM (Fig. 3b) or 1 μM (Fig. 3c) for 24 h.

3.5. BaP induced ROS production in NHEKs via AhR signaling pathway

To assess whether or not BaP-induced ROS production is AhR-CYP1A1 dependent, we examined the effect of AhR or CYP1A1 knockdown on BaP-induced ROS production in NHEKs. NHEKs transfected with siRNA targeted against scramble control (si-control), AhR (si-AhR(1), si-AhR(2)) or CYP1A1 (si-CYP(1), si-CYP(2)) were exposed to BaP (1 μM) for 24 h. Compared to NHEKs transfected with si-control (Fig. 4a), BaP-induced ROS production was strongly inhibited in NHEKs transfected with either si-AhR (1) (Fig. 4b), si-AhR (2) (Fig. 4c) or si-CYP (1) (Fig. 4d), si-CYP (2) (Fig. 4e) indicating that BaP-induced ROS production in NHEKs is strongly dependent on AhR signaling pathway. After transfection with siRNA for 48 h, we confirmed that transfection with si-AhR or si-CYP1A1 successfully knockdowned expression of AhR or CYP1A1 mRNA in NHEKs by RT-PCR analysis.

3.6. BaP induced IL-8 production in a dose-dependent manner

Since ROS play an important role in modulating cyto/chemokine production [8,9,17], we next measured the secretion of proinflammatory cyto/chemokines such as IL-1α, IL-6, IL-8, TNF-α and GM-CSF in culture supernatants of NHEKs by ELISA. In the presence of BaP (1 μM) for 24 h, IL-8 production was significantly augmented, whereas the production of IL-1α, IL-6, TNF-α and GM-CSF was not affected (Fig. 5a). In addition, IL-8 production was up-regulated in a dose-dependent manner by BaP exposure (Fig. 5b).

3.7. BaP-induced IL-8 production was ROS- and AhR-dependent

To examine whether or not BaP-induced IL-8 production is mediated via AhR signaling pathway, NHEKs transfected with si-control, si-AhR (1), or si-AhR (2) were exposed to BaP (1 μM) for 24 h and then production of IL-8 in culture supernatant were measured by ELISA. The BaP-induced augmentation of IL-8 production from NHEKs was cancelled by transfection with si-AhR (1) and si-AhR (2), indicating the critical role of AhR in BaP-induced IL-8 production (Fig. 6a). Since intracellular ROS levels are shown to be closely related to IL-8 production [9,17], we examined whether or not one of ROS inhibitors, NAC or catalase down-regulates the BaP-induced IL-8 production. NHEKs were pretreated with NAC (15 mM) or catalase (500 units/ml) for 2 h before

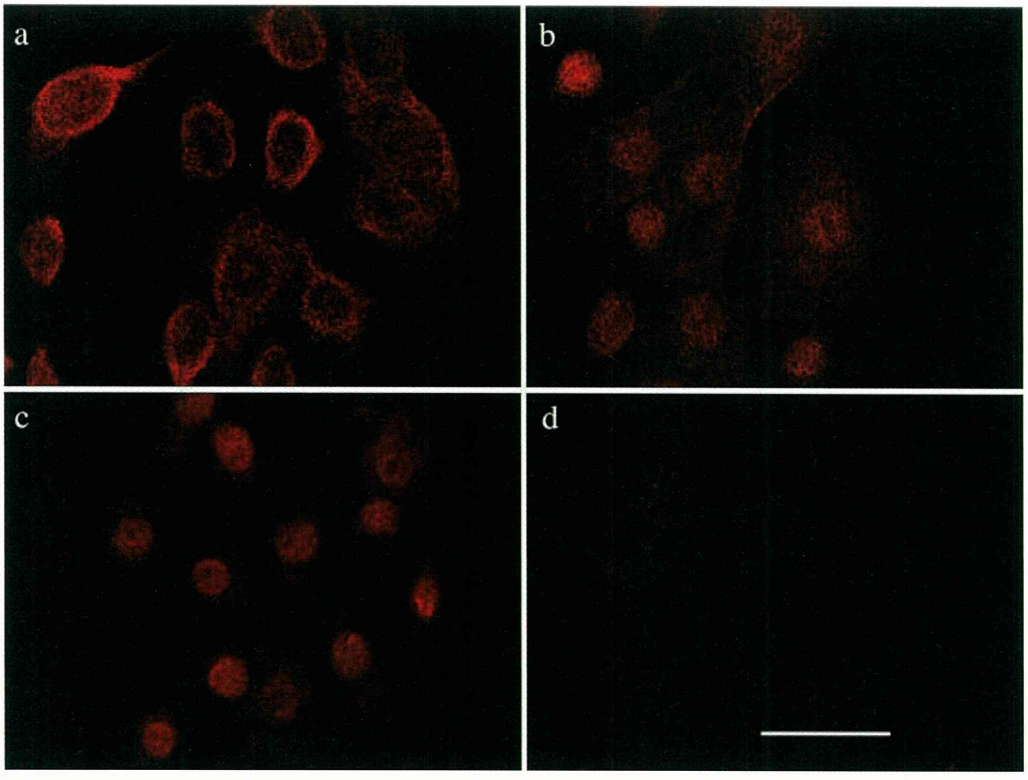

Fig. 1. Nuclear translocation of AhR from cytoplasm in NHEKs induced by BaP exposure. NHEKs were exposed to BaP (1 μM) for 3 h or 6 h. After BaP exposure, the distribution of AhR was observed by confocal laser scanning microscopy. (a) Under normal conditions (DMSO-treatment), AhR was localized in the cytoplasm. (b) AhR was observed not only in cytoplasm but also in nucleus at 3 h. (c) Consequently, AhR staining was observed mainly in the nucleus at 6 h. The data shown here is representative of experiments repeated three times with similar results. (d) Staining with rabbit iso-type, IgG used as a negative control. (Red: AhR) Scale bar = 50 μm.

exposure to BaP and were exposed to BaP (1 μM) for 24 h. NAC or catalase inhibited BaP-induced ROS production successfully (Fig. 6b). In accordance with these results, the addition of NAC or catalase completely abrogated the BaP-induced IL-8 production (Fig. 6c). These results indicate that the engagement of AhR by BaP induces downstream CYP1A1 expression together with subsequent ROS production, leading to the specific up-regulation of IL-8 production.

4. Discussion

PAHs including BaP are widely distributed in the environment, and the skin covering the outermost surface of the body must be the largest organ affected by PAHs externally and/or internally. However, only a few studies have focused on the metabolism and biology of PAHs in NHEKs [18–20]. The present study demonstrated the nuclear translocation of AhR from cytoplasm after BaP

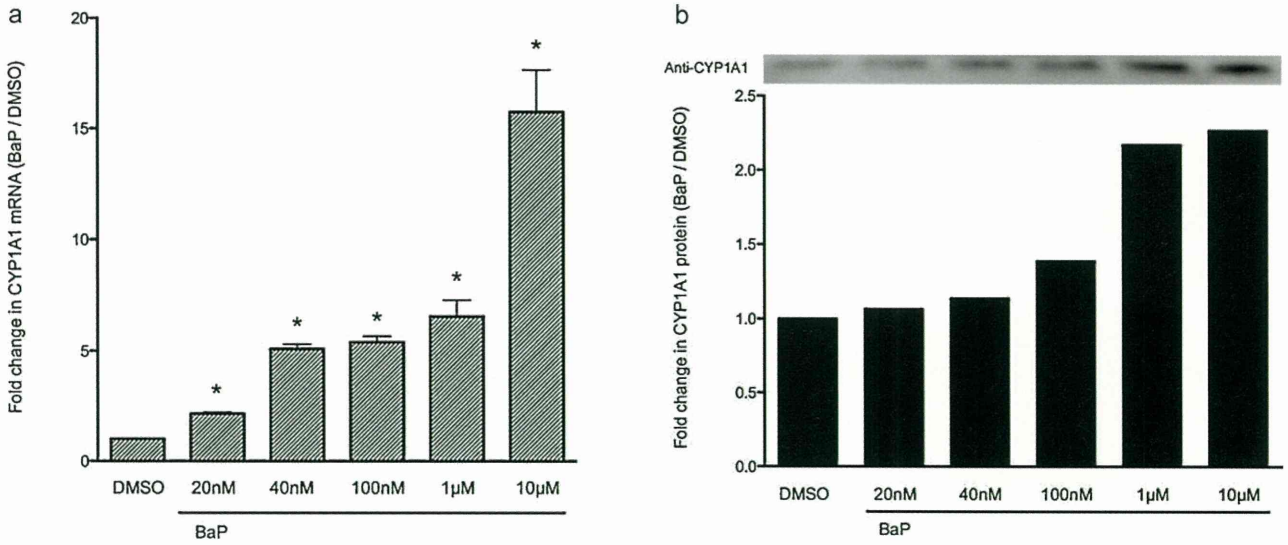

Fig. 2. BaP induced CYP1A1 mRNA and protein expression in NHEKs. (a) qRT-PCR analysis. NHEKs were incubated for 3 h with BaP in various concentrations. CYP1A1 mRNA levels were normalized for GAPDH mRNA levels. Data is expressed as fold induction of relevant mRNAs compared to the DMSO-treatment (control) group. Representative results (means in tripricates ± SD) from three separate experiments are shown. $^{*}p < 0.05$ compared to DMSO-treatment (control) (b) Western blotting analysis. NHEKs exposed to BaP for 24 h were lysated. The CYP1A1 protein levels were evaluated by visualizing on autoradiography and densitometric image analysis was performed using ImageJ software. The CYP1A1 mRNA and protein expression were induced by BaP in a dose-dependent manner. The data shown here is a representative of experiments with similar results.

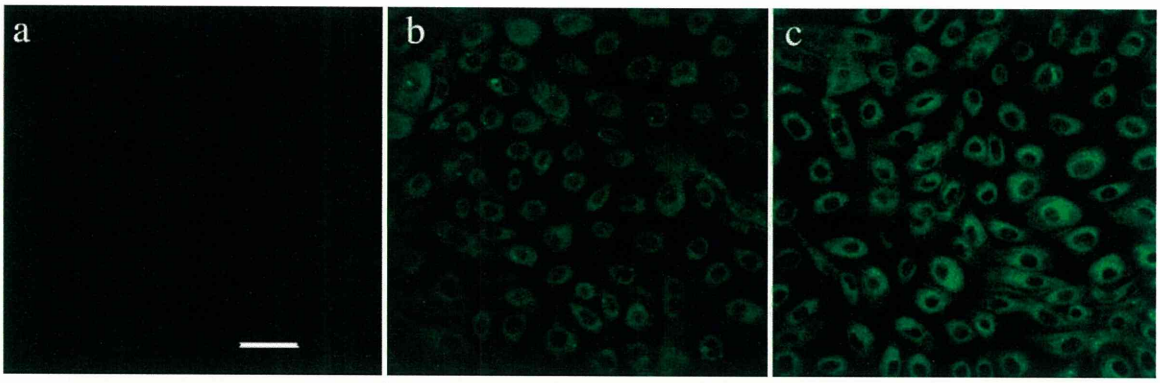

Fig. 3. BaP induced ROS production in a dose-dependent manner. Confocal laser scanning microscopic analysis. NHEKs on glass chamber slides were exposed to DMSO (control) or BaP (100 nM or 1 μM) for 24 h. As described in Section 2, NHEKs were incubated with DCFH-DA, which is a cell-permeable non-fluorescent probe that rapidly oxidized to highly fluorescent 2′,7′-dichlorofluorescein (DCF) in the presence of ROS. Green fluorescence intensity that reflected intracellular ROS (especially hydrogen peroxide) was detected by confocal laser scanning microscope. Compared to DMSO-treated NHEKs (control) (a), BaP induced ROS production in a dose-dependent manner (b); BaP 100 nM, (c); BaP 1 μM). Scale bar = 50 μm.

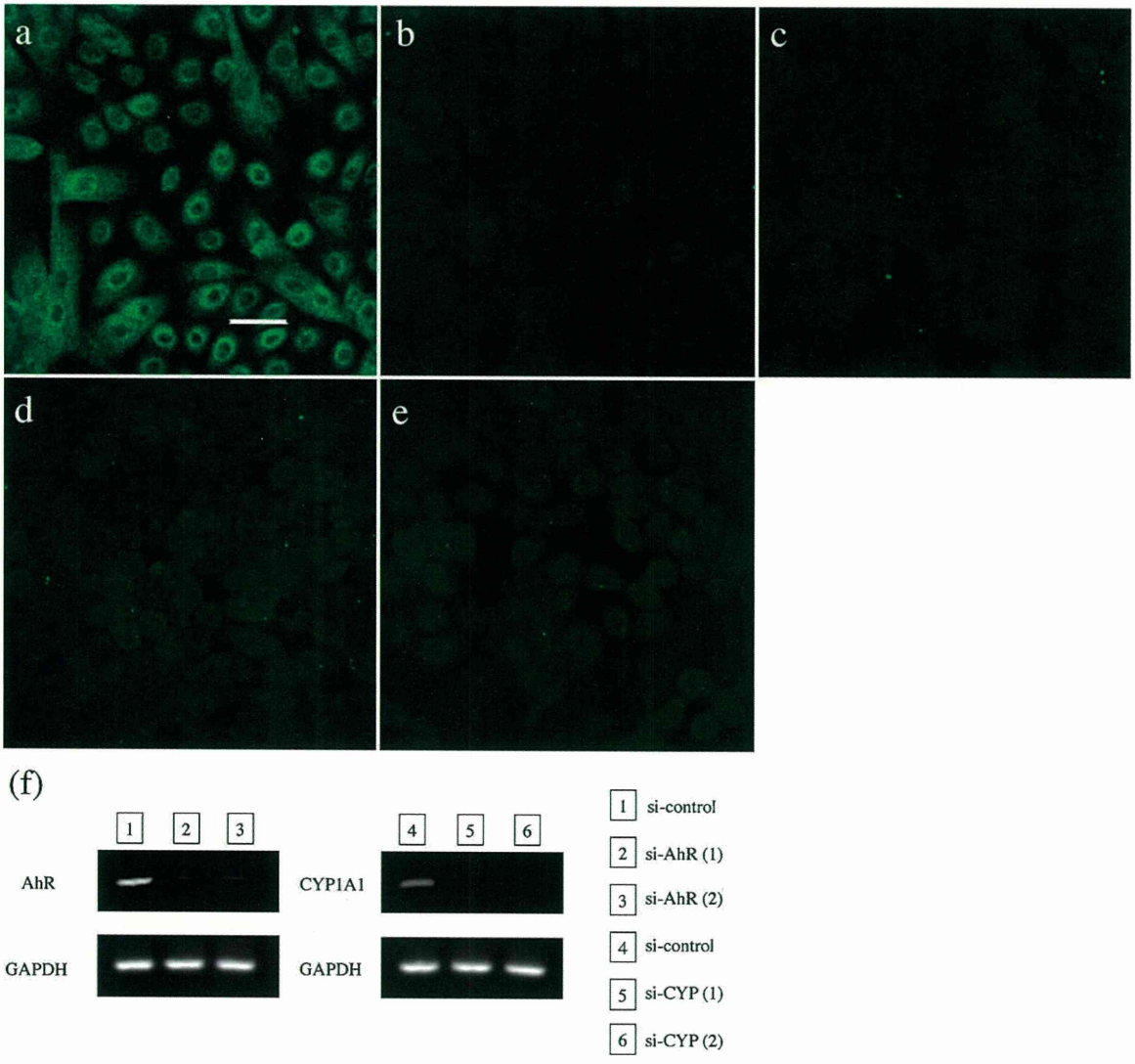

Fig. 4. BaP induced ROS production in NHEKs via AhR signaling pathway. NHEKs transfected with siRNA targeted against scramble control (si-control), AhR (si-AhR (1)), (si-AhR (2)) or CYP1A1 (si-CYP (1)), (si-CYP (2)) were exposed to BaP (1 μM) for 24 h. Compared to NHEKs transfected with si-control (a), BaP-induced ROS production was strongly inhibited in NHEKs transfected with either si-AhR (1) (b), si-AhR (2) (c) or si-CYP (1) (d), si-CYP (2) (e). Scale bar = 50 μm. (f) RT-PCR analysis confirmed that siRNA transfection against AhR or CYP1A1 successfully knockdowned expression of AhR or CYP1A1 mRNA in NHEKs. The data is representative of experiments repeated three times with similar results.

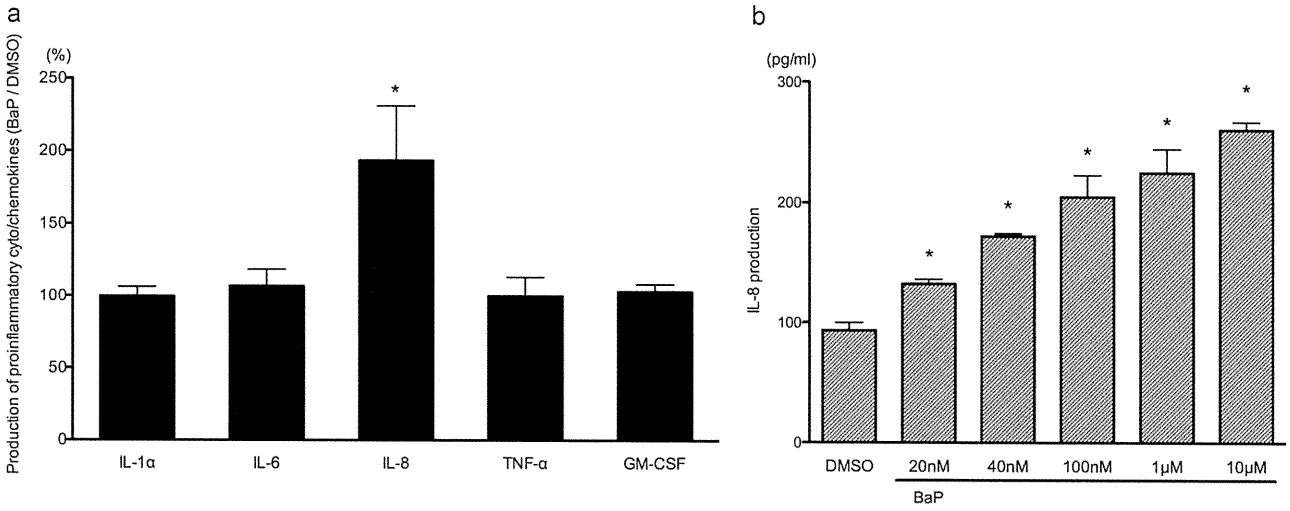

Fig. 5. BaP induced IL-8 production in a dose-dependent manner. (a) After treatment NHEKs with BaP (1 μM) for 24 h, the production of proinflammatory cytokines, IL-1α, IL-6, IL-8, TNF-α and GM-SCF in culture supernatant were measured by ELISA. We considered the cytokine production in DMSO-treatment group as a 100%. IL-8 production was significantly up-regulated compared to the DMSO-treatment (control) group; however, IL-1α, IL-6, IL-8, TNF-α and GM-SCF were not affected. $^*p < 0.05$ compared to DMSO-treatment (control) (b) NHEKs were exposed to BaP in various concentrations for 24 h, and then IL-8 production in culture supernatant was measured. BaP induced IL-8 production in a dose-dependent manner. The data represents the mean ± SD of three separate experiments. $^*p < 0.05$ compared to DMSO-treatment (control).

exposure in NHEKs. The engagement of AhR by its ligand, BaP, induced the expression of downstream CYP1A1 mRNA and protein in a dose-dependent manner with BaP, indicating that BaP is capable of activating AhR signaling pathways in NHEKs. Recent study reported that 5 μM BaP can significantly increase AhR and CYP1A1 expression and induce oxidative stress in human skin [21], which is consistent with our results. We further indicated that BaP in a low concentration is capable of activating AhR signaling in NHEKs. The doses of BaP utilized for in vitro assays to demonstrate systemic toxicity of inhalated tobacco smoke remain controversial, because BaP levels in blood is highly influenced by various factors such as lipoprotein [22] and lipid level [23]. Furthermore, metabolite of BaP is detectable in blood [24], indicating that BaP levels in blood might not be a good parameter in vitro assay. Several studies have utilized concentrations (200 nM–10 μM) of BaP as a systemic BaP exposure to human endothelial cell [25], monocyte [25] and primary cortical neuron [26]. To our knowledge, there is no study showing BaP concentration in human skin of smokers. Serum levels of BaP in smokers have been reported in only one study showing the concentrations of BaP in the serum (0.98 ± 0.56 ng/ml: equivalent to about 4–6 nM) and follicular fluid (1.79 ± 0.86 ng/ml) of the limited number of the women exposed to side stream [27]. However, the concentrations shown in this study were not examined at the highest time point. Accordingly, we considered that 20 nM which is 10-folds lower than previous studies is adequate to be a BaP concentration of inhaled tobacco smoking.

To investigate the proinflammatory effects of BaP on NHEKs, we focused on ROS production because it occurs via the metabolizing process of BaP by CYP1A1 [4,28] and there is compelling evidence that ROS drives the production of oxidative products, which can denature proteins and influence the release of proinflammatory cyto/chemokines, which may be critical for the induction of some inflammatory skin diseases [8,9,17,29]. Furthermore, it is also recognized that ROS can act as a second messenger in the initiation of signal transduction, such as the activation of NF-kB (nuclear factor kappa-light-chain-enhancer of activated B cells) or AP-1 (activator protein 1) and the production of proinflammatory cyto/chemokines [30]. The recent demonstration that the peroxisome proliferator-activated receptors, whose natural ligands are poly-unsaturated fatty acids and their oxidation products may be involved in the pathogenesis of psoriasis or acne, has further strengthened the concept that ROS can drive the development of these disorders [31]. The present study has revealed that ROS production was markedly up-regulated by BaP in a dose-dependent manner, which was inhibited in AhR or CYP1A1-knockdowned NHEKs. These results imply that ROS production induced by BaP is tightly dependent on the AhR signaling pathway.

Among the various proinflammatory cyto/chemokines examined, IL-8 was the only one that was sensitively up-regulated by BaP stimulation in a dose-dependent manner. Perez et al. have revealed that BaP exposure (2 μM) for 24 h up-regulated expression of IL-1α using microarray analysis [32]. This result may partly support our data, because IL-1 signaling regulates IL-8 gene expression in NHEKs [33]. However, BaP exposure (1 μM) for 24 h did not induce IL-1α production in protein level in our system, probably because BaP concentration is lower, and insufficient to induce up-regulation of IL-1α protein. The enhancing capacity of BaP in IL-8 production was again dependent on AhR, since the AhR-knockdowned NHEKs failed to augment their IL-8 production. Similar BaP-induced IL-8 production via AhR signaling pathway was recently reported in human monocyte-derived macrophages [34]. Since previous studies have already reported that intracellular ROS levels are closely related to IL-8 production in human keratinocytes [9,17], we examined whether or not up-regulation of IL-8 production by NHEKs was inhibited by treatment with NAC, one of ROS inhibitors, and confirmed that ROS is involved in BaP-induced IL-8 production. NAC has been shown to inhibit ROS production directly by scavenging ROS and also indirectly by supplying cysteine for the synthesis of the endogenous antioxidant GSH [35,36]. To prove the effect of ROS on IL-8 production, we examined experiments using catalase which functions to catalyze the decomposition of ROS [28,37]. Pretreatment with catalase inhibited BaP-induced IL-8 production (Fig. 6c), indicating that BaP-induced ROS generation is responsible for the IL-8 production. The molecular mechanism of IL-8 production has been investigated in various cell types, demonstrating that the IL-8 gene contains regulatory elements for NF-kB and AP-1, and among them NF-kB plays a key role in the induction of IL-8 expression [38,39]. Recent studies have revealed crosstalk between AhR and NF-kB [40,41]. AhR translocated into nucleus interacts with RelB which is NF-kb subunit and bind to an unrecognized RelB/AhR responsive element of IL-8 promoter [41]. This pathway can be another candidate for the mechanism of IL-8 induction. However, TCDD, a different ligand of AhR, was used in this model, which may induce a distinct biological response via AhR signaling [42]. Indeed, natural

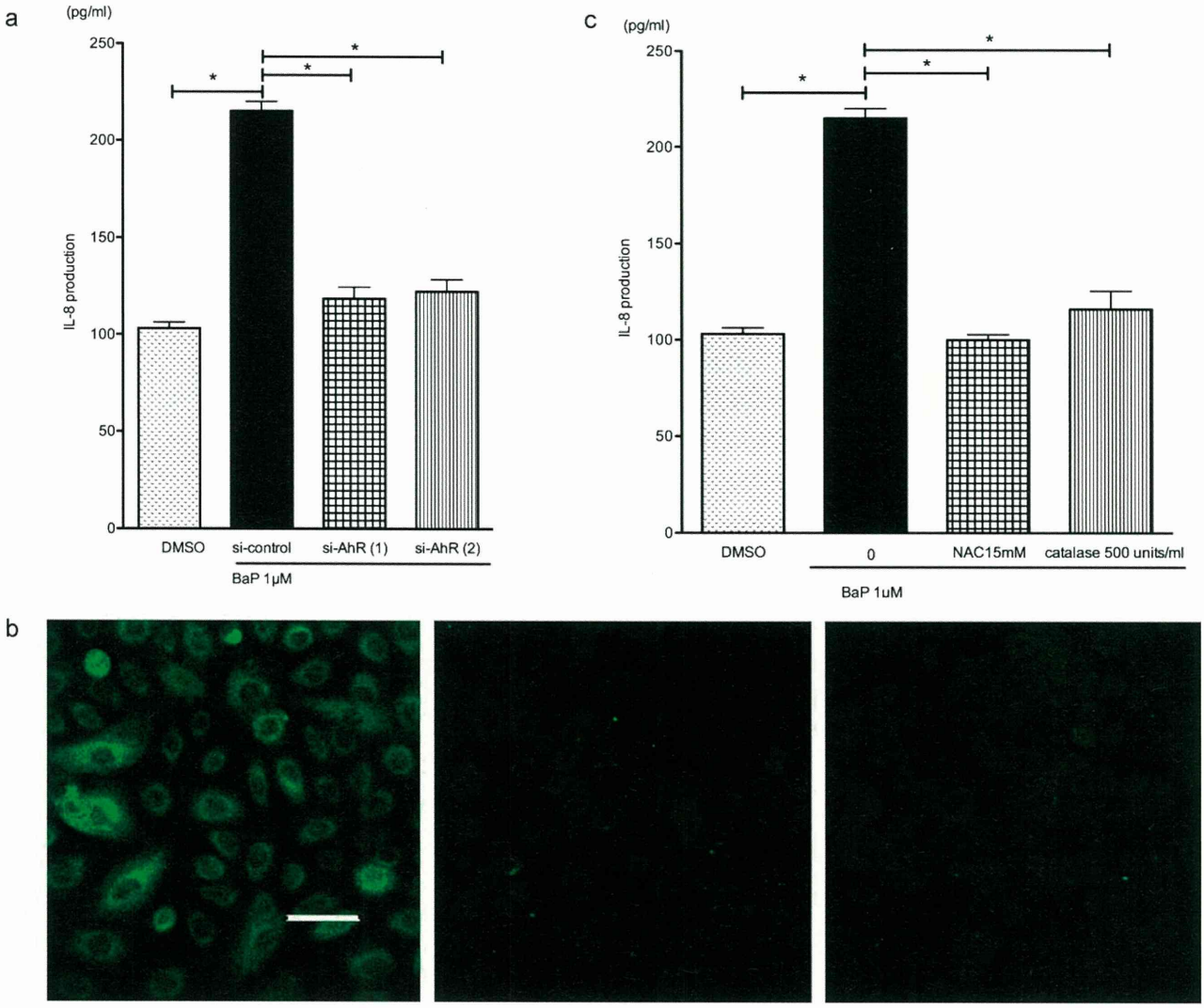

Fig. 6. BaP-induced IL-8 production was ROS-and AhR dependent. (a) NHEKs transfected with si-control, si-AhR (1), and si-AhR (2) were exposed to BaP (1 μM) for 24 h and production of IL-8 in culture supernatant was measured by ELISA analysis. The BaP-induced augmention of IL-8 production in NHEKs was completely cancelled by transfection with si-AhR (1) and si-AhR (2). The data represents the mean ± SD of three separate experiments. $^*p < 0.05$ compared to DMSO-treatment (control).(b) NHEKs were exposed to BaP (1 μM) in the absence (left panel) or presence of NAC (15 mM) (middle panel), or catalase (500 units/ml) (right panel) for 24 h. NAC and catalase clearly reduced the intracellular ROS levels. The data is representative of experiments repeated three times with similar results. Scale bar = 50 μm. (c) NHEKs were exposed to BaP (1 μM) in the presence of NAC (15 mM) or catalase (500 units/ml) for 24 h and BaP and IL-8 production in culture supernatant was measured. BaP-induced augmentation of IL-8 production was completely abrogated by NAC and catalase. The data represents the mean ± SD of three separate experiments. $^*p < 0.05$ compared to DMSO-treatment (control).

ligand such as resveratrol and curcumin inhibit NF-kb activation although they induce translocation of AhR into nuclei [18,43–45]. These findings suggest that further studies are required to elucidate the precise mechanism of RelB/AhR-mediated IL-8 production. Our data supports that ROS generation and cellular redox status can be involved in the activation of NF-kB, which leads to the expression of proinflammatory cyto/chemokines [38,39,46,47]. Among the various proinflammatory cyto/chemokines, IL-8 may be the most sensitive indicator responding to intracellular ROS intensity stimulated via AhR signaling.

IL-8 is one of the major cyto/chemokines in inflammatory response and activates the recruitment and function of neutrophils [48]. The pathogenetic role of IL-8 has been postulated, at least in part, in neutrophil-related skin diseases such as psoriasis [49,50], palmoplantar pustulosis [50] and acne [48,51,52]. *Propionibacterium acnes* is feasible for inducing IL-8 production in various cell types including NHEKs [52,53]. A major symptom of toxicity by PAHs such as 2,3,7,8-tetrachlorodibenzo-p-dioxin and polychlorinated dibenzofurans is chloracne [54]. Dioxin-induced IL-8 production by NHEKs may contribute to the development and exacerbation of chloracne. Interestingly, tabacco smoking is considered an aggravating factor in these IL-8 related skin diseases by epidemiological studies [10,55]. Some reports have shown that severity in patients with psoriasis [11,12] or acne [13] is correlated with the smoking habits of patients. Fortes et al. [11] showed that patients with psoriasis are at a more than 2-fold increased risk for severer disease activity when smoking intensively. Schäfer et al. [13] described a significant dose-dependent relationship between acne severity and daily tabacco consumption. Exacerbation of palmoplantar pustulosis is also correlated with smoking [14–16]. Considering that BaP is a major PAH contained in tobacco smoke, the BaP-AhR-ROS-dependent IL-8 up-regulation in NHEKs may explain, at least in part, why tobacco smoking aggravates IL-8 related skin diseases.

Acknowledgments

This study was supported by a grant from the Ministry of Health, Labour and Welfare, Japan and the Environmental Technology Development Fund of the Ministry of the Environment, Japan.

References

[1] Gough M. Human health effects: what the data indicate. Sci Total Environ 1991;104:129–58.
[2] Chen SC, Liao CM. Health risk assessment on humans exposed to environmental polycyclic aromatic hydrocarbons pollution sources. Sci Total Environ 2006;366:112–23.
[3] Bagdon RE, Hazen RE. Skin permeation and cutaneous hypersensitivity as a basis for making risk assessments of chromium as a soil contaminant. Environ Health Perspect 1991;92:111–9.
[4] Nebert DW, Dalton TP, Okey AB, Gonzalez FJ. Role of aryl hydrocarbon receptor-mediated induction of the CYP1 enzymes in environmental toxicity and cancer. J Biol Chem 2004;279:23847–50.
[5] Mandal PK. Dioxin: a review of its environmental effects and its aryl hydrocarbon receptor biology. J Comp Physiol B 2005;175:221–30.
[6] Burczynski ME, Lin HK, Penning TM. Isoform-specific induction of a human aldo-keto reductase by polycyclic aromatic hydrocarbons (PAHs), electrophiles, and oxidative stress: implications for the alternative pathway of PAH activation catalyzed by human dihydrodiol dehydrogenase. Cancer Res 1999;59:607–14.
[7] Ma Q, Lu AY. Origins of individual variability in P4501A induction. Chem Res Toxicol 2003;16:249–60.
[8] Thannickal VJ, Fanburg BL. Reactive oxygen species in cell signaling. Am J Physiol Lung Cell Mol Physiol 2000;279:1005–28.
[9] Young CN, Koepke JI, Terlecky LJ, Borkin MS, Boyd Savoy L, Terlecky SR. Reactive oxygen species in tumor necrosis factor-alpha-activated primary human keratinocytes: implications for psoriasis and inflammatory skin disease. J Invest Dermatol 2008;128:2606–14.
[10] Jankovic S, Raznatovic M, Marinkovic J, Jankovic J, Maksimovic N. Risk factors for psoriasis: a case–control study. J Dermatol 2009;36:328–34.
[11] Fortes C, Mastroeni S, Leffondré K, Sampogna F, Melchi F, Mazzotti E, et al. Relationship between smoking and the clinical severity of psoriasis. Arch Dermatol 2005;141:1580–4.
[12] Gerdes S, Zahl VA, Weichenthal M, Mrowietz U. Smoking and alcohol intake in severely affected patients with psoriasis in Germany. Dermatology 2010;220:38–42.
[13] Schäfer T, Nienhaus A, Vieluf D, Berger J, Ring J. Epidemiology of acne in the general population: the risk of smoking. Br J Dermatol 2001;145:100–4.
[14] Akiyama T, Seishima M, Watanabe H, Nakatani A, Mori S, Kitajima Y. The relationship of onset and exacerbation of pustulosis palmaris et plantaris to smoking and focal infection. J Dermatol 1995;22:930–4.
[15] Douwes KE, Karrer S, Abels C, Landthaler M, Szeimies R-M. Does smoking influence the efficacy of bath-PUVA therapy in chronic palmoplantar eczema? Photodermatol Photoimmunol Photomed 2000;16:25–9.
[16] Miot HA, Miot LDB, Lopes PS, Haddad GR, Marques SA. Association between palmoplantar pustulosis and cigarette smoking in Brazil: a case–control study. J Eur Acad Dermatol Venereol 2009;23:1173–7.
[17] Kang JS, Kim HN, Jung da J, Kim JE, Mun GH, Kim YS, et al. Regulation of UVB-induced IL-8 and MCP-1 production in skin keratinocytes by increasing vitamin C uptake via the redistribution of SVCT-1 from the cytosol to the membrane. J Invest Dermatol 2006;27:698–706.
[18] Du L, Neis MM, Ladd PA, Keeney DS. Differentiation-specific factors modulate epidermal CYP1-4 gene expression in human skin in response to retinoic acid and classic aryl hydrocarbon receptor ligands. J Pharmacol Exp Ther 2006;319:1162–71.
[19] Reiners Jr JJ, Jones CL, Hong N, Myrand S. Differential induction of Cyp1a1, Cyp1b1, Ahd4, and Nmo1 in murine skin tumors and adjacent normal epidermis by ligands of the aryl hydrocarbon receptor. Mol Carcinog 1998;21:135–46.
[20] Shimizu Y, Nakatsuru Y, Ichinose M, Takahashi Y, Kume H, Mimura J, et al. Benzo[a]pyrene carcinogenicity is lost in mice lacking the aryl hydrocarbon receptor. Proc Natl Acad Sci USA 2000;97:779–82.
[21] Costa C, Catania S, De Pasquale R, Stancanelli R, Scribano GM, Melchini A. Exposure of human skin to benzo[a]pyrene: role of CYP1A1 and aryl hydrocarbon receptor in oxidative stress generation. Toxicology 2010;27:83–6.
[22] Shu HP, Nichols AV. Benzo(a)pyrene uptake by human plasma lipoproteins in vitro. Cancer Res 1979;39:1224–30.
[23] Curfs DM, Beckers L, Godschalk RW, Gijbels MJ, van Schooten FJ. Modulation of plasma lipid levels affects benzo[a]pyrene-induced DNA damage in tissues of two hyperlipidemic mouse models. Environ Mol Mutagen 2003;42:243–9.
[24] Shinozaki R, Inoue S, Choi KS, Tatsuno T. Association of benzo[a]pyrene-diol-epoxide-deoxyribonucleic acid (BPDE-DNA) adduct level with aging in male smokers and nonsmokers. Arch Environ Health 1999;54:79–85.
[25] Vayssier-Taussat M, Camilli T, Aron Y, Meplan C, Hainaut P, Polla BS, et al. Effects of tobacco smoke and benzo[a]pyrene on human endothelial cell and monocyte stress responses. Am J Physiol Heart Circ Physiol 2001;280:H1293–300.
[26] Dutta K, Ghosh D, Nazmi A, Kumawat KL, Basu A. A common carcinogen benzo[a]pyrene causes neuronal death in mouse via microglial activation. PLoS One 2010;5:e9984.
[27] Neal MS, Zhu J, Foster WG. Quantification of benzo[a]pyrene and other PAHs in the serum and follicular fluid of smokers versus non-smokers. Reprod Toxicol 2008;25:100–6.
[28] Shyong EQ, Lu Y, Goldstein A, Lebwohl M, Wei H. Synergistic enhancement of H_2O_2 production in human epidermoid carcinoma cells by benzo[a]pyrene and ultraviolet A radiation. Toxicol Appl Pharmacol 2003;188:104–9.
[29] Trenam CW, Dabbagh AJ, Blake DR, Morris CJ. The role of iron in an acute model of skin inflammation induced by reactive oxygen species (ROS). Br J Dermatol 1992;126:250–6.
[30] Briganti S, Picardo M. Antioxidant activity, lipid peroxidation and skin diseases. What's new. J Eur Acad Dermatol Venereol 2003;17:663–9.
[31] Okayama Y. Oxidative stress in allergic and inflammatory skin diseases. Curr Drug Targets Inflamm Allergy 2005;4:517–9.
[32] Perez DS, Handa RJ, Yang RS, Campain JA. Gene expression changes associated with altered growth and differentiation in benzo[a]pyrene or arsenic exposed normal human epidermal keratinocytes. J Appl Toxicol 2008;28:491–508.
[33] Yano S, Banno T, Walsh R, Blumenberg M. Transcriptional responses of human epidermal keratinocytes to cytokine interleukin-1. J Cell Physiol 2008;214:1–13.
[34] Podechard N, Lecureur V, Ferrec EL, Guenon I, Sparfel L, Gilot D, et al. Interleukin-8 induction by environmental contaminant benzo(a)pyrene is aryl hydrocarbon receptor-dependent and leads to lung inflammation. Toxicol Lett 2008;177:130–7.
[35] Morley N, Curnow A, Salter L, Campbell S, Gould D. N-acetyl-L-cysteine prevents DNA damage induced by UVA, UVB and visible radiation in human fibroblasts. J Photochem Photobiol B 2003;72:55–60.
[36] Park LJ, Ju SM, Song HY, Lee JA, Yang MY, Kang YH, et al. The enhanced monocyte adhesiveness after UVB exposure requires ROS and NF-kappaB signaling in human keratinocyte. J Biochem Mol Biol 2006;39:618–25.
[37] Rezvani HR, Mazurier F, Cario-André M, Pain C, Ged C, Taïeb A, et al. Protective effects of catalase overexpression on UVB-induced apoptosis in normal human keratinocytes. J Biol Chem 2006;28:17999–8007.
[38] Mukaida N, Okamoto S, Ishikawa Y, Matsushima K. Molecular mechanism of interleukin-8 gene expression. J Leukoc Biol 1994;5:554–8.
[39] Sarir H, Mortaz E, Janse WT, Givi ME, Nijkamp FP, Folkerts G. IL-8 production by macrophage is synergistically enhanced when cigarette smoke is combined with TNF-α. Biochem Pharmacol 2010;79:698–705.
[40] Zordoky BN, El-Kadi AO. Role of NF-kappaB in the regulation of cytochrome P450 enzymes. Curr Drug Metab 2009;10:164–78.
[41] Vogel CF, Matsumura F. A new cross-talk between the aryl hydrocarbon receptor and RelB, a member of the NF-kappaB family. Biochem Pharmacol 2009;77:734–45.
[42] Beischlag TV, Luis Morales J, Hollingshead BD, Perdew GH. The aryl hydrocarbon receptor complex and the control of gene expression. Crit Rev Eukaryot Gene Expr 2008;18:207–50.
[43] Nam NH. Naturally occurring NF-kappaB inhibitors. Mini Rev Med Chem 2006;6(August (8)):945–51.
[44] Cho JW, Lee KS, Kim CW. Curcumin attenuates the expression of IL-1beta, IL-6, and TNF-alpha as well as cyclin E in TNF-alpha-treated HaCaT cells; NF-kappaB and MAPKs as potential upstream targets. Int J Mol Med 2007;19:469–74.
[45] Rinaldi AL, Morse MA, Fields HW, Rothas DA, Pei P, Rodrigo KA, et al. Curcumin activates the aryl hydrocarbon receptor yet significantly inhibits (−)-benzo(a)pyrene-7R-trans-7,8-dihydrodiol bioactivation in oral squamous cell carcinoma cells and oral mucosa. Cancer Res 2002;62:5451–6.
[46] Meyer M, Schreck R, Baeuerle PA. H_2O_2 and antioxidants have opposite effects on activation of NF-kappa B and AP-1 in intact cells: AP-1 as secondary antioxidant-responsive factor. EMBO J 1993;12:2005–15.
[47] Wilhelm D, Bender K, Knebel A, Angel P. The level of intracellular glutathione is a key regulator for the induction of stress-activated signal transduction pathways including Jun N-terminal protein kinases and p38 kinase by alkylating agents. Mol Cell Biol 1997;17:4792–800.
[48] Nakatsuji T, Liu YT, Huang CP, Zoubouis CC, Gallo RL, Huang CM. Antibodies elicited by inactivated *Propionibacterium acnes*-based vaccines exert protective immunity and attenuate the IL-8 production in human sebocytes: relevance to therapy for Acne vulgaris. J Invest Dermatol 2008;128:2451–7.
[49] Duan H, Koga T, Kohda F, Hara H, Urabe K, Furue M. Interleukin-8-positive neutrophils in psoriasis. J Dermatol Sci 2001;26:119–24.
[50] Anttila HS, Reitamo S, Erkko P, Ceska M, Moster B, Baggiolini M. Interleukin-8 immunoreactivity in the skin of healthy subjects and patients with palmoplantar pustulosis and psoriasis. J Invest Dermatol 1992;98:96–101.
[51] Lyte P, Sur R, Nigam A, Southall MD, Heat-killed. *Propionibacterium acnes* is capable of inducing inflammatory responses in skin. Exp Dermatol 2009;18:1070–2.
[52] Chen Q, Koga T, Uchi H, Hara H, Terao H, Moroi Y, et al. *Propionibacterium acnes*-induced IL-8 production may be mediated by NF-kappaB activation in human monocytes. J Dermatol Sci 2002;29:97–103.
[53] Grange PA, Chéreau C, Raingeaud J, Nicco C, Weill B, Dupin N, et al. Production of superoxide anions by keratinocytes initiates P. acnes-induced inflammation of the skin. PLoS Pathog 2009;(July (5)):e1000527. Epub 2009 July 24.
[54] Imamura T, Kanagawa Y, Matsumoto S, Tajima B, Uenotsuchi T, Shibata S, et al. Relationship between clinical features and blood levels of pentachlorodibenzofuran in patients with Yusho. Environ Toxicol 2007;22:124–31.
[55] Freiman A, Bird G, Metelitsa AI, Barankin B, Lauzon GJ. Cutaneous effects of smoking. J Cutan Med Surg 2004;8:415–23.

See related commentary on pg 7

ORIGINAL ARTICLE

Identification of Ketoconazole as an AhR-Nrf2 Activator in Cultured Human Keratinocytes: The Basis of Its Anti-Inflammatory Effect

Gaku Tsuji[1,3], Masakazu Takahara[1,3], Hiroshi Uchi[1,2], Tetsuo Matsuda[1], Takahito Chiba[1,2], Satoshi Takeuchi[1], Fumiko Yasukawa[1,2], Yoichi Moroi[1] and Masutaka Furue[1,2]

Ketoconazole (KCZ) has been shown to exhibit anti-inflammatory effects in addition to its inhibitory effects against fungi; however, the underlying molecular mechanism remains poorly understood. Aryl hydrocarbon receptor (AhR), a receptor that is activated by polycyclic aromatic hydrocarbons (PAHs) and halogenated aromatic hydrocarbons such as dioxin, is a sensor of the redox system against oxidative stress and regulates nuclear factor-erythroid 2-related factor-2 (Nrf2), a master switch of the redox machinery. To clarify whether KCZ modulates AhR-Nrf2 function leading to redox system activation, cultured human keratinocytes were treated with KCZ. Confocal microscopic analysis revealed that KCZ induced AhR nuclear translocation, resulting in the upregulation of CYP1A1 mRNA and protein expression. Furthermore, KCZ actively switched on Nrf2 nuclear translocation and quinone oxidoreductase 1 expression. Tumor necrosis factor-α- and benzo(a)pyrene (BaP)-induced reactive oxidative species (ROS) and IL-8 production were effectively inhibited by KCZ. Knockdown of either AhR or Nrf2 abolished the inhibitory capacity of KCZ on ROS and IL-8 production. In addition, KCZ-induced Nrf2 activation was canceled by AhR knockdown. Moreover, KCZ inhibited BaP-induced 8-hydroxydeoxyguanosine and IL-8 production. In conclusion, the engagement of AhR by KCZ exhibits the cytoprotective effect mediated by the Nrf2 redox system, which potently downregulates either cytokine-induced (AhR-independent) or PAH-induced (AhR-dependent) oxidative stress.

Journal of Investigative Dermatology (2012) **132,** 59–68; doi:10.1038/jid.2011.194; published online 14 July 2011

INTRODUCTION

Ketoconazole (KCZ) is an azole antifungal agent. KCZ may be particularly effective against inflammatory skin diseases, including psoriasis (Farr *et al.*, 1985), acne (De Pedrini *et al.*, 1988), and atopic dermatitis (Bäck *et al.*, 1995). The mechanism by which KCZ inhibits skin inflammation has largely depended on its suppression of *Malassezia* spp, which contributes to the aggravation of seborrheric dermatitis (Gupta *et al.*, 2004) and atopic dermatitis (Darabi *et al.*, 2009). However, KCZ also exerts a direct anti-inflammatory effect (Kanda and Watanabe, 2006; Nakashima *et al.*, 2007), the mechanism of which has remained largely unknown.

Several studies of oral KCZ-induced hepatic dysfunction have revealed that KCZ induces aryl hydrocarbon receptor (AhR) signaling-mediated genes in human hepatocytes (Casley *et al.*, 2007; Korashy *et al.*, 2007). AhR is activated by polycyclic aromatic hydrocarbons (PAHs) and halogenated aromatic hydrocarbons such as dioxin. Specifically, AhR signaling occurs as follows (Ma and Lu, 2003): (1) the ligand interacts with AhR in the cytoplasm; (2) the ligand–AhR complex translocates from the cytoplasm into the nucleus; (3) the ligand–AhR complex forms a heterodimer ligand/AhR/AhR nuclear translocator in the nucleus; and (4) the ligand/AhR/AhR nuclear translocator complex binds to xenobiotic response elements and activates the transcription of some members of the cytochrome P450 enzyme family such as CYP1A1, which metabolizes and activates the ligand. Previous studies, including our report, have shown that AhR signaling in normal human epidermal keratinocytes (NHEKs) functions as a metabolizing system for PAHs such as benzo(a)pyrene (BaP; Khan *et al.*, 1992; Tsuji *et al.*, 2011).

Furthermore, AhR signaling has a cross-talk with other transcription factors (Köhle and Bock, 2007; Haarmann-Stemmann *et al.*, 2009). In the present study, we focused on

[1]*Department of Dermatology, Graduate School of Medical Sciences, Kyushu University, Fukuoka, Japan and* [2]*Research and Clinical Center for Yusho and Dioxin, Kyushu University Hospital, Fukuoka, Japan*

[3]*These authors contributed equally to this work.*

Correspondence: Gaku Tsuji, Department of Dermatology, Graduate School of Medical Sciences, Kyushu University, 3-1-1 Maidashi, Higashi-ku, Fukuoka 812-8582, Japan. E-mail: gakku@dermatol.med.kyushu-u.ac.jp

Abbreviations: 8-OHdG, 8-hydroxydeoxyguanosine; AhR, aryl hydrocarbon receptor; AhRR, aryl hydrocarbon receptor repressor; ARE, antioxidant response elements; BaP, benzo(a)pyrene; KCZ, ketoconazole; NHDF, normal human dermal fibroblast; NHEK, normal human epidermal keratinocyte; Nqo1, NAD(P)H:quinone acceptor oxidoreductase 1; Nrf2, nuclear factor-erythroid 2-related factor-2; PAH, polycyclic aromatic hydrocarbon; RES, resveratrol; ROS, reactive oxygen species; TBF, terbinafine hydrochloride; TNF-α, tumor necrosis factor-α

Received 10 November 2010; revised 29 April 2011; accepted 13 May 2011; published online 14 July 2011

nuclear factor-erythroid 2-related factor-2 (Nrf2), which is a key molecule responsible for turning on the protective systems for cell damage. Nrf2 is anchored to Kelch-like ECH-associated protein 1 in the cytoplasm. When the Nrf2–Kelch-like ECH-associated protein 1 complex is disrupted by an inducer, Nrf2 translocates from the cytoplasm into the nucleus to bind antioxidant response elements (AREs). ARE-mediated induction of antioxidant enzymes, including NAD(P)H:quinone oxidoreductase 1 (Nqo1), is critical for protection from cell damage caused by reactive oxygen species (ROS; Jaiswal, 2004).

Therefore, we hypothesized that KCZ may exert its anti-inflammatory effects on inflammatory skin diseases by activating Nrf2 via AhR signaling. To prove this, cultured NHEKs were treated with KCZ. We demonstrated that KCZ (1) activates AhR signaling in NHEKs, (2) activates Nrf2 via AhR signaling, and (3) inhibits tumor necrosis factor-α (TNF-α)- or BaP-induced ROS and IL-8 production via AhR-Nrf2.

RESULTS

KCZ, terbinafine hydrochloride, BaP, and resveratrol do not affect NHEK viability

Cell viability was determined by Trypan blue dye exclusion. Incubation with KCZ (10 nM–1 μM), terbinafine hydrochloride (TBF; 1 μM), BaP (1 μM), and resveratrol (RES; 1 μM) for 48 hours showed no effect on the viability or morphological features of NHEKs (data not shown), as described previously (Kanda and Watanabe, 2006).

KCZ activates AhR signaling in NHEKs

To determine whether KCZ activates AhR signaling, we examined AhR nuclear translocation. NHEKs were treated with DMSO (control), KCZ (1 μM), or TBF (1 μM), a non-azole antifungal agent, for 6 hours. Confocal laser scanning micro scopy revealed that AhR was mainly localized in the cytoplasm under unstimulated condition (DMSO treatment; Figure 1a). Following KCZ treatment, AhR staining was observed mainly in the nuclei (Figure 1b), indicating that KCZ induces AhR nuclear translocation in NHEKs. In contrast, TBF treatment did not affect AhR distribution (Figure 1c) even after 24 hours (data not shown).

Next, we examined whether KCZ induced CYP1A1 expression by quantitative real-time PCR (qRT-PCR) and western blotting analysis. NHEKs were treated with KCZ (1 μM) for 3, 6, 24, and 48 hours for qRT-PCR analysis and for 24 and 48 hours for western blotting analysis. KCZ induced CYP1A1 mRNA and protein upregulation (Figure 1e and f). Furthermore, NHEKs were treated with different doses of KCZ (10 nM, 100 nM, and 1 μM) for 3 hours, because AhR began to translocate into the nuclei at this point (data not shown). KCZ induced the upregulation of CYP1A1 mRNA in a dose-

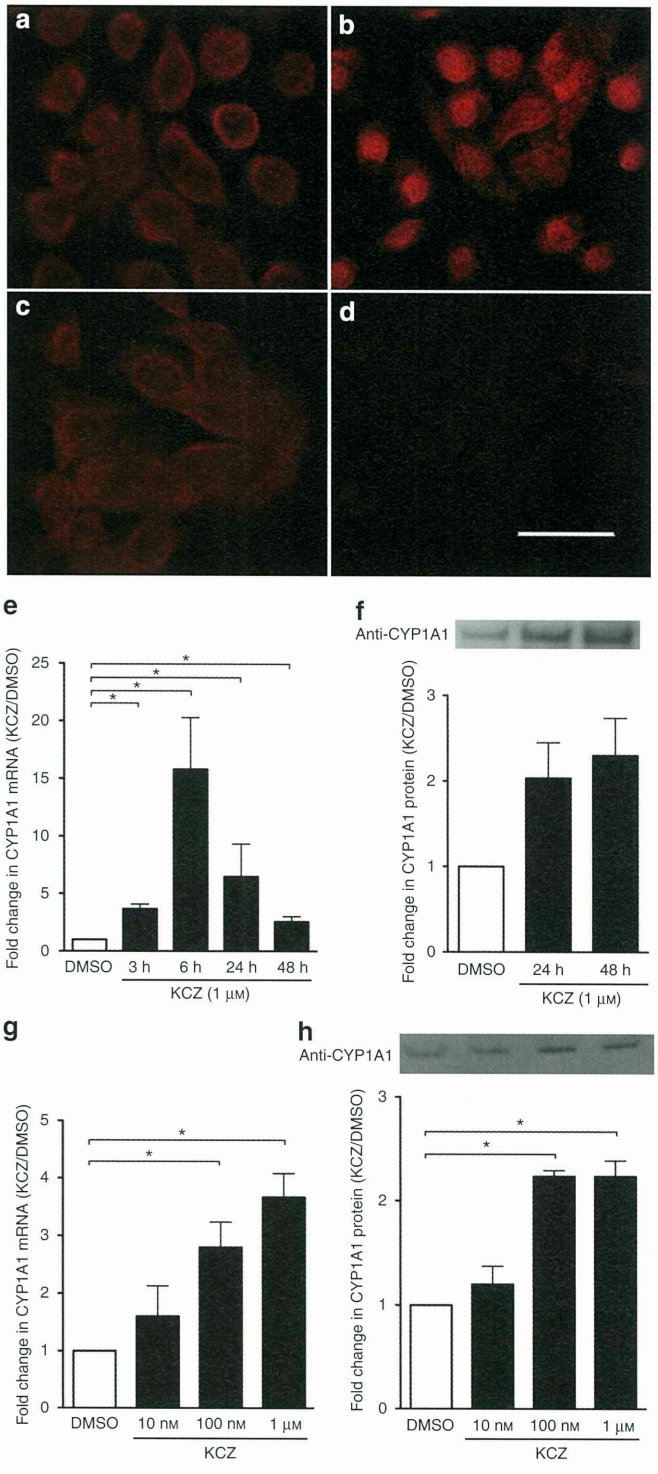

Figure 1. Ketoconazole (KCZ) activated aryl hydrocarbon receptor signaling in normal human epidermal keratinocytess. Confocal laser scanning microscopic analysis. (**a**) DMSO treatment (control), (**b**) KCZ (1 μM), (**c**) terbinafine hydrochloride (1 μM) treatment for 6 hours, and (**d**) isotype negative control. Bar = 50 μm. Representative data, $n = 3$ (**a**–**d**). (**e**, **g**) Quantitative real-time PCR analysis. Treatment with 1 μM KCZ for 3, 6, 24, and 48 hours or with 10 nM, 100 nM, and 1 μM KCZ for 3 hours. CYP1A1 mRNA levels normalized for glyceraldehyde-3-phosphate dehydrogenase (GAPDH) mRNA levels were expressed as fold induction compared with DMSO group. (**f**, **h**) Western blotting analysis. Treatment with 1 μM KCZ for 24 and 48 hours or with 10 nM, 100 nM, and 1 μM KCZ for 24 hours. CYP1A1 protein levels were normalized for GAPDH protein levels using ImageJ. Means ± SD, ($n = 3$) (**e**–**h**). *$P < 0.05$ (**e**–**h**).

dependent manner (Figure 1g). Western blotting analysis confirmed that KCZ induced the upregulation of CYP1A1 protein in NHEKs treated with KCZ (100 nM and 1 μM) for 24 or 48 hours (Figure 1h).

KCZ activates Nrf2 signaling in NHEKs

To elucidate whether KCZ activates Nrf2 in NHEKs, we examined Nrf2 distribution. NHEKs were treated with DMSO (control) or KCZ (1 μM) for 12 hours. Under unstimulated condition (DMSO treatment), Nrf2 was mainly localized in the cytoplasm (Figure 2a). Following KCZ treatment, Nrf2 staining was observed mainly in the nuclei (Figure 2b), indicating that KCZ induces Nrf2 nuclear translocation.

Next, we examined whether KCZ induced Nrf2 and Nqo1 upregulation. NHEKs were treated with KCZ for 12 hours for qRT-PCR analysis and for 24 hours for western blotting analysis. KCZ induced Nrf2 and Nqo1 mRNA and protein upregulation in a dose-dependent manner (Figure 2d and e).

Furthermore, ELISA-based Nrf2 transcriptional assay, which detects whether Nrf2 protein interacted with an oligonucleotide in ARE, confirmed that KCZ-induced nuclear Nrf2 bound to ARE (Figure 2f).

Nrf2 activation by KCZ requires AhR signaling in NHEKs

To examine whether KCZ activates Nrf2 via AhR signaling, AhR was knocked down by small interference (si)RNA transfection. After transfection with siRNA control (si-control) or siRNA against AhR (si-AhR) for 48 hours, NHEKs were treated with KCZ (1 μM) or BaP (1 μM) for 12 hours. KCZ induced Nrf2 nuclear translocation in si-control-transfected NHEKs (Figure 3a); however, in si-AhR-transfected NHEKs, the KCZ-induced Nrf2 nuclear translocation was completely abolished (Figure 3b). In addition, BaP induced Nrf2 upregulation in si-control-transfected NHEKs, which was inhibited in si-AhR-transfected NHEKs. However, BaP did not induce Nrf2 nuclear translocation (Supplementary Figure S1 online). Si-AhR transfection successfully knocked down AhR expression at the protein level (Figure 3d).

AhR and Nrf2 are responsible for the inhibitory effect of KCZ on TNF-α-induced ROS–IL-8 production

To evaluate the inhibitory effect of KCZ on inflammation, we used TNF-α to induce ROS-mediated IL-8 production in NHEKs (Young *et al.*, 2008). After treatment with DMSO (control) or KCZ (1 μM) for 48 hours, NHEKs were exposed to TNF-α (10 ng ml^{-1}) for 30 minutes. ROS production was evaluated using 2′,7′-dichlorofluorescein diacetate (DCFH-DA). DMSO (control; Figure 4a) and KCZ (1 μM) treatment for 6, 24, and 48 hours (Figure 4b) did not induce visible ROS production (Supplementary Figure S2 online). In contrast, TNF-α markedly induced ROS production in DMSO-treated NHEKs (control; Figure 4c), but not when NHEKs were treated with KCZ (Figure 4d).

Next, we examined whether KCZ exerted this anti-inflammatory effect by AhR-mediated gene expression, including AhR, Nrf2, and aryl hydrocarbon receptor repressor (AhRR) genes. AhRR functions as a negative feedback to AhR signaling, which inhibits CYP1A1 upregulation (Mimura *et al.*, 1999). TNF-α did not affect AhRR mRNA expression and KCZ-induced CYP1A1 upregulation (Supplementary Figure S3 online). siRNA transfection successfully knocked down Nrf2 expression at the protein level (Figure 3d) and AhRR expression at the mRNA level (Figure 4i). KCZ (1 μM) inhibited TNF-α-induced ROS in si-control (Figure 4e) or si-AhRR (Figure 4h)-transfected NHEKs, which was canceled in si-AhR (Figure 4f) or si-Nrf2 (Figure 4g)-transfected NHEKs.

Furthermore, we examined the effect of KCZ on IL-8 production (Figure 4, Supplementary Figure S4 online). After KCZ (100 nM, 1 μM) treatment for 48 hours, NHEKs were exposed to TNF-α (50 ng ml^{-1}) for 3 hours. KCZ inhibited TNF-α-induced IL-8 production in the culture supernatant in a dose-dependent manner (Figure 4j). More importantly, AhR or Nrf2 knockdown, but not AhRR knockdown, canceled this inhibitory effect on TNF-α-induced IL-8 production (Figure 4k).

KCZ inhibits BaP-induced oxidative stress in NHEKs

We hypothesized that KCZ might inhibit oxidative stress induced by AhR agonists, including PAHs and dioxins antagonistically, because KCZ also activates AhR signaling. After KCZ (100 nM, 1 μM) or DMSO (control) treatment for 48 hours, NHEKs were exposed to BaP (1 μM) for 24 hours. KCZ and BaP did not affect AhRR mRNA expression (Supplementary Figure S3 online). BaP induced ROS production in NHEKs (Figure 5b), which was inhibited by KCZ treatment (Figure 5c). Furthermore, Nrf2 (Figure 5e), but not AhRR (Figure 5f), knockdown canceled the inhibitory effect of KCZ on BaP-induced ROS production. Next, we examined whether KCZ inhibited BaP-induced IL-8 upregulation (Figure 5g, Supplementary Figure S4 online). KCZ (100 nM and 1 μM) inhibited BaP-induced IL-8 production in a dose-dependent manner (Figure 5g). Furthermore, we examined nuclear 8-hydroxydeoxyguanosine (8-OHdG) production resulting from DNA damage induced by ROS (Saladi *et al.*, 2003). KCZ (1 μM) treatment for 48 hours did not induce 8-OHdG production (data not shown). BaP (1 μM) exposure for 24 hours induced 8-OHdG production in DMSO-treated NHEKs (control), which was significantly inhibited by KCZ (100 nM, 1 μM) in a dose-dependent manner (Figure 5h).

DISCUSSION

The present study has provided the first evidence that KCZ induces Nrf2 activation in cultured human keratinocytes through AhR-dependent mechanisms. Specifically, we have demonstrated that KCZ induces Nrf2 nuclear translocation and promotes Nrf2 binding to ARE, leading to Nqo1 upregulation. Nqo1 is a relevant marker for Nrf2 activation (Marrot *et al.*, 2008), implying KCZ as an Nrf2 inducer and activator.

Our studies using siRNA targeted against AhR revealed that AhR is required to initiate Nrf2 translocation after KCZ treatment (Figure 3a and b). Recent data have provided lines of evidence regarding the cross-talk between AhR signaling and Nrf2, leading to the induction of antioxidant enzymes in human hepatocytes (Yeager *et al.*, 2009). They have suggested two possible mechanisms by which AhR signaling

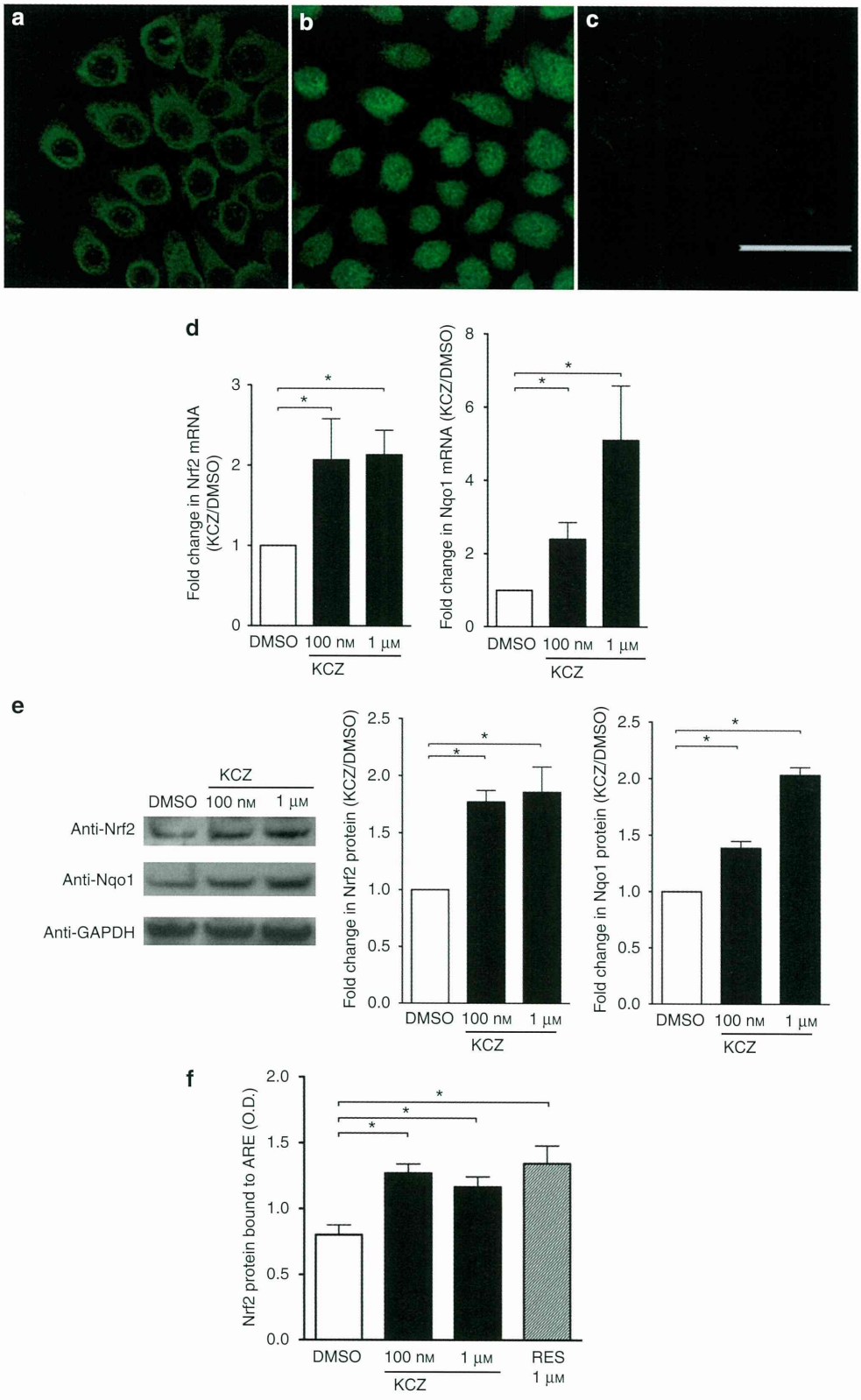

Figure 2. Ketoconazole (KCZ) activated nuclear factor-erythroid-2-related factor-2 (Nrf2) in normal human epidermal keratinocytes. Confocal laser scanning microscopic analysis. (**a**) DMSO treatment (control). (**b**) Treatment with 1 μM KCZ for 12 hours. (**c**) Isotype negative control. Bar = 50 μm. Representative data, $n = 3$ (**a**–**c**). (**d**) Quantitative real-time PCR analysis. Treatment with 100 nM and 1 μM KCZ for 12 hours. Nrf2 or Nqo1 mRNA levels normalized for glyceraldehyde-3-phosphate dehydrogenase (GAPDH) mRNA levels were expressed as fold induction compared with the DMSO group. (**e**) Western blotting analysis. Treatment with 100 nM and 1 μM KCZ for 24 hours. Protein levels were normalized for GAPDH protein levels using ImageJ. (**f**) ELISA-based Nrf2 transcriptional analysis. Protein levels of nuclear Nrf2, which interacted with an oligonucleotide in antioxidant response elements were measured. Data are presented as means ± SD, $n = 3$ (**d**–**f**). *$P < 0.05$ (**d**–**f**).

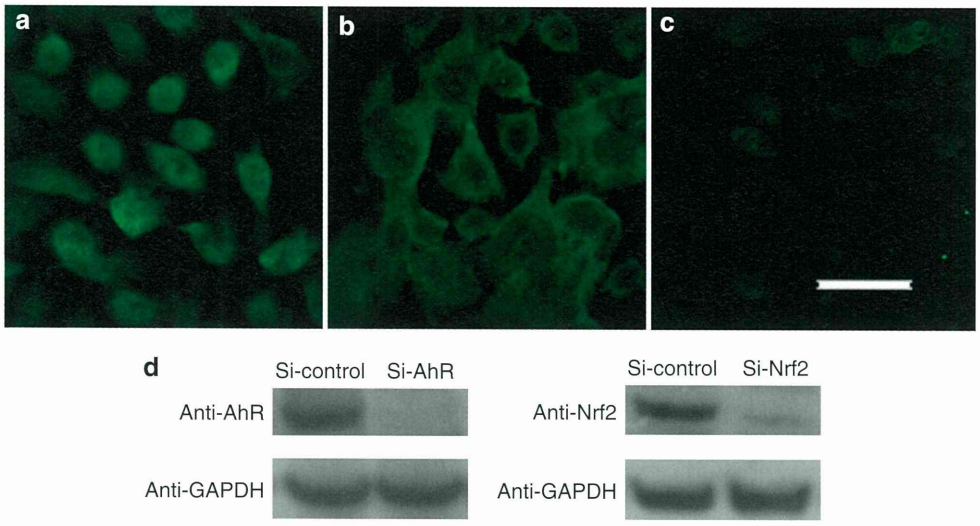

Figure 3. Ketoconazole (KCZ) activated nuclear factor-erythroid-2-related factor-2 (Nrf2) via aryl hydrocarbon receptor (AhR) signaling in normal human epidermal keratinocytes (NHEKs). After transfection with small interference (si) RNA control (si-control) or siRNA against AhR (si-AhR) for 48 hours, NHEKs were treated with 1 μM KCZ for 12 hours. Nrf2 distribution was observed by confocal laser scanning microscopy. (**a**) Si-control-transfected NHEKs. KCZ induced Nrf2 nuclear translocation as described in Figure 2b. (**b**) Si-AhR-transfected NHEKs. KCZ-induced Nrf2 nuclear translocation was completely abolished. (**c**) Isotype negative control. Bar = 50 μm. (**d**) Western blotting analysis. Si-AhR or si-Nrf2 transfection successfully knocked down AhR or Nrf2 expression at the protein level, respectively. Representative data, $n = 3$ (**a**–**d**). GAPDH, glyceraldehyde-3-phosphate dehydrogenase; RES, resveratrol.

activates Nrf2: (1) ROS production caused by CYP1A1 metabolism of a ligand would facilitate Nrf2 nuclear translocation and (2) AhR might bind to the Nrf2 gene locus and increase Nrf2 transcription as suggested by Miao *et al.* (2005). Our results possibly support the latter mechanism, because KCZ treatment did not induce ROS production (Figure 4b, Supplementary Figure S2 online). Although we showed that KCZ induced AhR nuclear translocation and CYP1A1 expression, we did not confirm the binding between KCZ and AhR in NHEKs. KCZ has been shown to directly bind to AhR and induce AhR nuclear translocation in human hepatocytes (Korashy *et al.*, 2007), indicating that KCZ may be a, to our knowledge, previously unreported AhR ligand. In addition, Henry and Gasiewicz (2008) have determined specific amino acids within AhR ligand-binding domains, showing that non-dioxin chemicals bind to AhR. These previous reports strongly suggest that KCZ activates AhR signaling in NHEKs through the direct engagement of KCZ to AhR.

Next, we have demonstrated that KCZ exerts an anti-inflammatory effect against TNF-α- or BaP-induced oxidative stress. Similar results that KCZ inhibits ROS released by primed inflammatory cells (Nakashima *et al.*, 2007) and TNF-α-induced CCL27, CCL12, and CCL5 production in NHEKs (Kanda and Watanabe, 2006) have been reported; however, the underlying molecular mechanism remains unknown. The present study has identified that AhR and Nrf2, but not AhRR, are critical in the anti-inflammatory effect of KCZ in NHEKs. The mRNA expression of AhRR, a negative feedback to AhR activation (Mimura *et al.*, 1999), was not affected by KCZ, TNF-α, and BaP (Supplementary Figure S3 online). Indeed, AhRR mRNA expression in NHEKs was much lower than that in HeLa cells and normal human dermal fibroblasts (NHDFs; Supplementary Figure S3 online; Tsuchiya *et al.*, 2003; Akintobi *et al.*, 2007), suggesting that AhRR does not modulate AhR activation sufficiently in NHEKs.

Results from AhR activation differ with cell types and AhR ligands. Whether AhR activation inhibits inflammation, including IL-8 expression, has remained controversial. In keratinocytes, AhR ligands affect responses of AhR activation strongly. 6-Formylindolo[3,2-b]carbazole, a tryptophan derivate, and 2,3,7,8-tetrachlorodibenzodioxin induce inflammation by AhR-mediated cyclooxygenase-2 induction (Fritsche *et al.*, 2007), whereas curcumin, a potent AhR activator (Rinaldi *et al.*, 2002), induces cyclooxygenase-2 inhibition (Nandal *et al.*, 2009). Furthermore, AhR translocated into nuclei by 2,3,7,8-tetrachlorodibenzodioxin exposure interacts with the NF-κ light-chain enhancer of the activated B-cell (NF-κB) subunit RelB and binds to a RelB/AhR-responsive element of IL-8 promoter (Vogel *et al.*, 2007). On the other hand, RES, which is another AhR ligand, inhibits NF-kB activation (Adhami *et al.*, 2003), although it induces AhR nuclear translocation (Casper *et al.*, 1999). Thus, the type of AhR ligand is an important factor in determining the response of AhR signaling. Some AhR ligands including RES (Liu *et al.*, 2011) and curcumin (Natarajan *et al.*, 2010) induce Nrf2 upregulation in human keratinocytes. Activation of Nrf2-antioxidant signaling attenuates NF-kB- or cyclooxygenase-2-induced inflammatory response (Li *et al.*, 2008; Hwang *et al.*, 2011). Therefore, we believe that the Nrf2 activation by AhR ligands contributes to the subsequent response of AhR signaling.

The property of KCZ to inhibit TNF-α-induced ROS and IL-8 production suggests that KCZ can be a therapeutic agent for various inflammatory skin diseases because ROS trigger the induction and maintenance of skin inflammation (Bickers and Athar, 2006) and IL-8 is a major proinflammatory

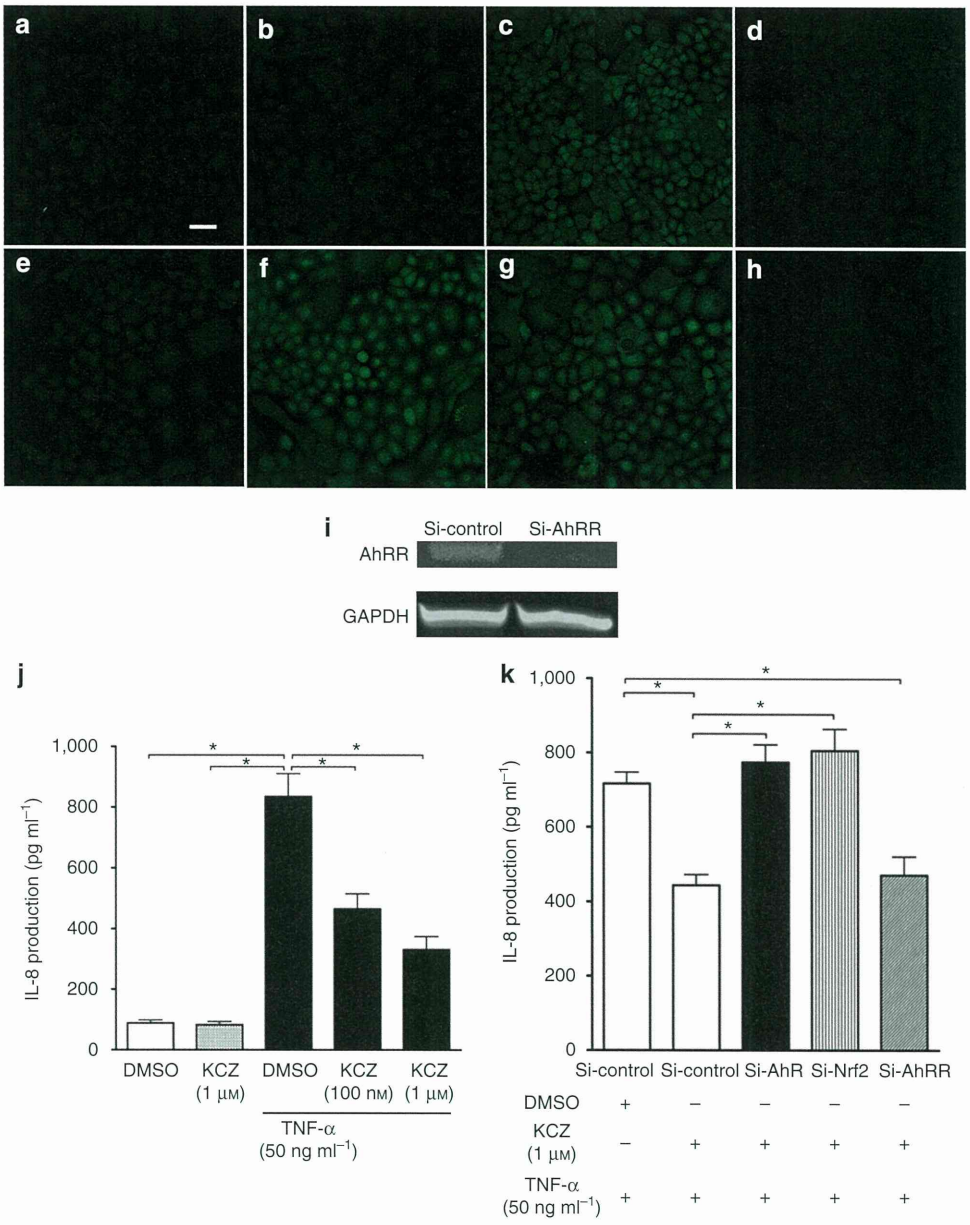

Figure 4. The inhibitory effect of ketoconazole (KCZ) on tumor necrosis factor-α (TNF-α)-induced reactive oxidative species (ROS)–IL-8 production required aryl hydrocarbon receptor (AhR) and nuclear factor-erythroid 2-related factor-2 (Nrf2). ROS production evaluation using 2′,7′-dichlorofluorescein diacetate. (**a**) DMSO (control), bar = 50 μm. (**b**) KCZ (1 μM, 48 hours). (**c**) TNF-α (10 ng ml^{-1}, 30 minutes) induced ROS production (**d**), but not in KCZ (100 nM, 48 hours)-pretreated normal human epidermal keratinocytes (NHEKs) (**e**). KCZ inhibited TNF-α-induced ROS production in si-control- (**e**) or si-aryl hydrocarbon receptor repressor (AhRR)- (**h**) transfected NHEKs, which was canceled in si-AhR- (**f**) or si-Nrf2- (**g**) transfected NHEKs. (**i**) Reverse transcription-PCR analysis. Small interference (si)-aryl hydrocarbon receptor repressor (AhRR) transfection successfully knocked down AhRR mRNA expression. Representative data, $n = 3$ (**a–i**). (**j**) KCZ pretreatment (48 h) inhibited tumor necrosis factor-α (TNF-α; 50 ng ml^{-1}, 3 hours)-induced IL-8 production in a dose-dependent manner. (**k**) KCZ inhibited TNF-α-induced IL-8 production in si-control- or si-AhRR-transfected NHEKs, but not in si-AhR- or si-Nrf2-transfected NHEKs. Data are presented as means ± SD, $n = 3$ (**j**, **k**). *$P < 0.05$ (**j**, **k**).GAPDH, glyceraldehyde-3-phosphate dehydrogenase.

cytokine/chemokine activating the recruitment and function of neutrophils (Baggiolini and Clark-Lewis, 1992). Furthermore, considering that AhR signaling is originally a metabolizing system for PAHs, we evaluated the property of KCZ to inhibit oxidative stress caused by an AhR agonist, including PAHs. KCZ inhibited BaP-induced ROS, IL-8, and 8-OHdG production (Figure 5c, d, g and h). 8-OHdG is a marker of DNA damage caused by ROS contributing to carcinogenesis (Saladi *et al.*, 2003). Elucidation of the precise molecular mechanism by which KCZ inhibits BaP-induced oxidative stress appears quite difficult in this system, because BaP also activates AhR signaling in NHEKs. However, Nrf2 knockdown restored the inhibitory effect of KCZ on BaP-induced ROS production, suggesting that Nrf2 possibly has an important role. These data suggest that KCZ may protect cells from AhR-mediated oxidative stress, including PAHs

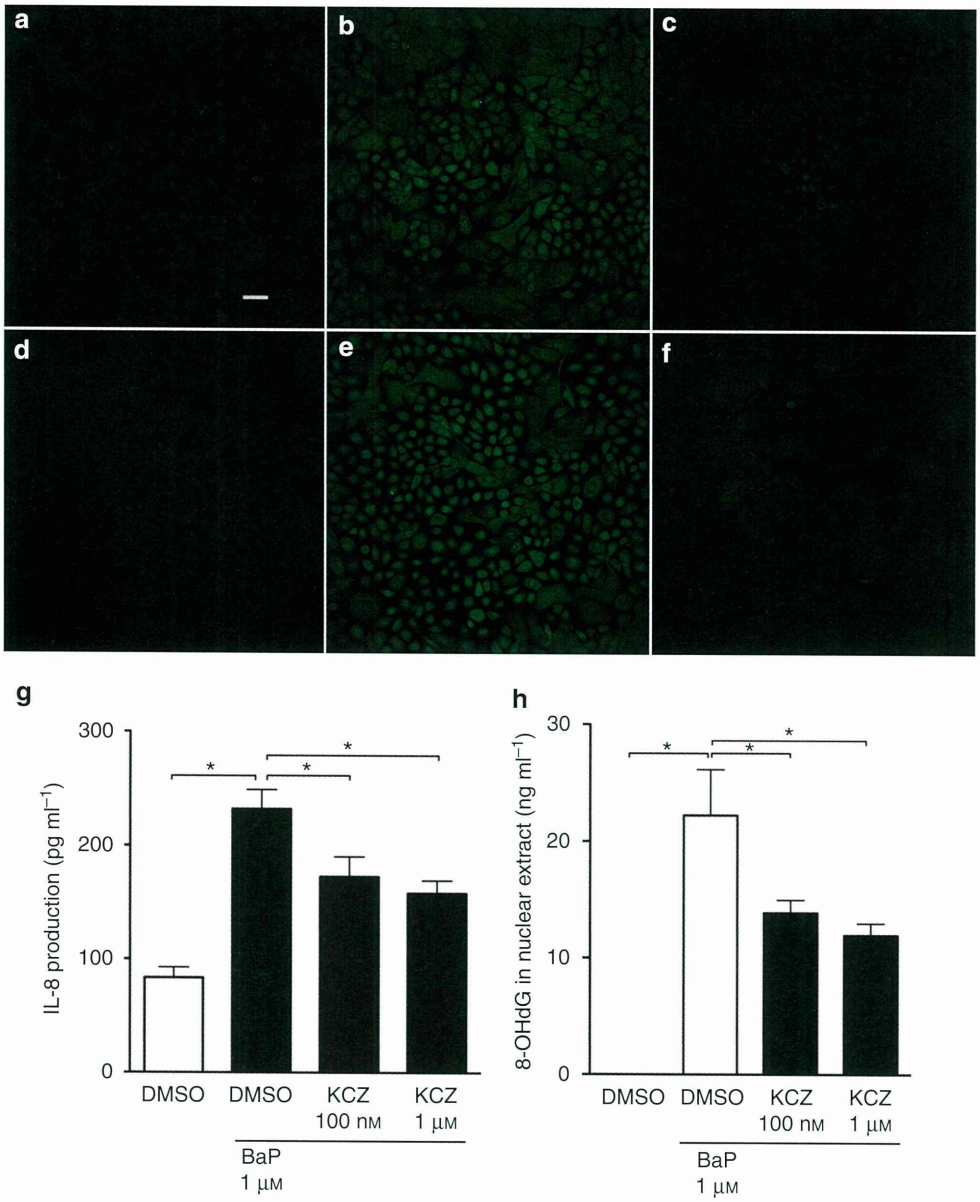

Figure 5. Ketoconazole (KCZ) inhibited benzo(a)pyrene (BaP)-induced reactive oxidative species (ROS)–IL-8 production in normal human epidermal keratinocytes (NHEKs). ROS production evaluation using 2′,7′-dichlorofluorescein diacetate. (**a**) DMSO (control), bar = 50 μm. BaP (1 μM) treatment for 24 hours induced ROS production (**b**), which was inhibited by KCZ (100 nM) pretreatment for 48 hour-treated NHEKs (**c**). Si-Nrf2 transfection (**e**) canceled this KCZ inhibition, but si-control (**d**) and small interference (si)-aryl hydrocarbon receptor repressor (**f**) transfection did not. Representative data, $n = 3$ (**a–f**). (**g**) ELISA: IL-8 production in culture supernatant. BaP induced IL-8 production in DMSO-treated NHEKs (control), which was inhibited by KCZ treatment in a dose-dependent manner. (**h**) ELISA: 8-hydroxydeoxyguanosine (8-OHdG) production in nuclear extract. BaP induced 8-OHdG production in DMSO (control)-treated NHEKs, which was inhibited by KCZ treatment in a dose-dependent manner. Data are presented as means ± SD, $n = 3$ (**g**, **h**). *$P < 0.05$ (**g**, **h**).
Nrf2, nuclear factor-erythroid 2-related factor-2.

and dioxin toxicity. As AhR-mediated oxidative stress is partly involved in clinical symptoms of dioxin-overexposed patients, including Yucheng (Wang *et al.*, 2008) and Yusho patients (Imamura *et al.*, 2007), KCZ treatment may have a possibility to improve these symptoms.

We found that 100 nM KCZ was sufficient to inhibit ROS and IL-8 production. The concentration of 100 nM is much lower than the peak serum concentration (7.2 μM) obtained from oral KCZ (200 mg) treatment (Chin *et al.*, 1995). As oral KCZ occasionally causes hepatic dysfunction, topical skin application is used more frequently, suggesting that the KCZ dose obtained from topical treatment is desirable for *in vitro* assay. However, to the best of our knowledge, there are still no studies that indicate the optimal KCZ dose based on topical treatment. Molecules with a molecular weight under 500 Da can penetrate normal skin (Bos and Meinardi, 2000). KCZ, having a molecular weight of 531 Da, may thus partially penetrate normal skin. However, KCZ absorption may be increased in an inflamed skin because the inflammation impairs the skin barrier function.

In conclusion, our findings suggest that engagement of AhR by KCZ induces the cytoprotective effect mediated by Nrf2 activation, which potently downregulates either cytokine-induced (AhR-independent) or PAH-induced (AhR-dependent) oxidative stress in cultured human keratinocytes.

MATERIALS AND METHODS

Regents and antibodies

KCZ, RES, TBF, BaP, and DMSO were purchased from Sigma Chemical (St Louis, MO). TNF-α was obtained from Peprotech (Rocky Hill, NJ). Anti-AhR rabbit polyclonal IgG antibody (H-211), anti-CYP1A1 mouse monoclonal IgG antibody (B-4), anti-Nrf2 polyclonal rabbit IgG antibody (H-300), anti-AhRR rabbit IgG antibody (D-14), anti-glyceraldehyde-3-phosphate dehydrogenase (GAPDH) rabbit IgG antibody (FL-335), normal rabbit IgG, and normal mouse IgG were obtained from Santa Cruz Biotechnology (Santa Cruz, CA). Anti-Nqo1 mouse monoclonal IgG (A180) was procured from Abcam (Cambridge, UK).

Cell culture

NHEKs, NHDFs, obtained from Clonetics-BioWhittaker (San Diego, CA), and HeLa cells (CCL-2, ATCC) were grown in culture dishes at 37 °C, 5% CO_2. NHEKs were cultured in serum-free keratinocyte growth medium (Lonza, Walkersville, MD) supplemented with bovine pituitary extract, recombinant epidermal growth factor, insulin, hydrocortisone, transferrin, and epinephrine. NHDFs and HeLa cells were cultured in DMEM supplemented with 10% fetal calf serum, 2 mM non-essential amino-acid solution, 2 mM pyruvate, and 2 mM HEPES buffer. Culture medium was replaced every 2 days. At near confluence (70–90%), cells were disaggregated with 0.25% trypsin/0.01% ethylenediamine tetraacetic acid and subcultured. Second-to-fourth-passage NHEKs or NHDFs were uszed in all experiments.

Treatment of cultured NHEKs

NHEKs (1×10^5) were seeded in 24-well culture plates, allowed to attach for 24 hours, and subsequently treated with KCZ, TBF, RES, BaP, TNF-α, or DMSO. Various concentrations of KCZ (10 nM, 100 nM and 1 μM), TBF (1 μM), RES (1 μM), BaP (1 μM), and TNF-α (10 or 50 ng ml^{-1}) were prepared in cell culture medium. Control cultures received medium containing a comparable DMSO concentration (up to 0.05%). Fresh medium containing KCZ, TBF, RES, BaP, TNF-α, or DMSO was added as indicated in the figure legend.

Immunofluorescence and confocal laser scanning microscopic analysis

NHEKs cultured on slides were washed in phosphate-buffered saline (PBS), fixed with acetone for 10 minutes, and blocked using 10% BSA in PBS for 30 minutes. Samples were incubated with primary rabbit anti-AhR (1:50) or rabbit anti-Nrf2 (1:50) in PBS overnight at 4 °C. Slides were washed in PBS before incubation with anti-rabbit (Alexa Fluor 488 or 546, Molecular Probes, Eugene, OR) secondary antibody for 1.5 hours at room temperature. Slides were mounted with ProLong Gold antifade reagent (Invitrogen, Carlsbad, CA). All samples were analyzed using D-Eclipse confocal laser scanning microscope (Nikon, Tokyo, Japan).

Reverse transcription-PCR and qRT-PCR analyses

Total RNA was extracted using RNeasy Mini kit (Qiagen, Valencia, CA). Reverse transcription was performed using PrimeScript RT-PCR kit (Takara Bio, Shiga, Japan). Amplification was started at 95 °C for 10 seconds as the first step, followed by 35 cycles of PCR at 95 °C for 5 seconds, and at 60 °C for 20 seconds. PCR products were analyzed using electrophoresis, and densitometric analysis was performed using ImageJ software (NIH). ImageJ is a public domain, Java-based image processing program developed at the National Institutes of Health (NIH; Bethesda, MD). qRT-PCR was performed on the Mx3000p real-time system (Stratagene, La Jolla, CA) using SYBR Premix Ex Taq (Takara Bio). The amplification protocol was the same as that with reverse transcription-PCR. mRNA expressions were measured in triplicate and were normalized for GAPDH expression levels. The primers from Takara Bio and SABiosciences (Frederick, MD) were as follows: AhR: forward 5′-ATCACCTACGCCAGTCGCA AG-3′ and reverse: 5′-AGGCTAGCCAAACGGTCCAAC-3′; Nrf2: forward 5′-CTTGGCCTCAGTGATTCTGAAGTG-3′ and reverse: 5′-C CTGAGATGGTGACAAGGGTTGTA-3′; Nqo1: forward 5′-GGATTG GACCGAGCTGGAA-3′ and reverse: 5′-AATTGCAGTGAAGATGAA GGCAAC-3′; AhRR: forward 5′-GCCTCTGGGCATTTATGGATTTA AG-3′ and reverse: 5′-CTGGGCACTCGGTTAGAATAGGAA-3′; IL-8: forward 5′-ACTTTCAGAGACAGCAGAGCACACA-3′ and reverse: 5′-CCTTCACACAGAGCTGCAGAAATC-3′; and GAPDH: forward 5′-GCACCGTCAAGGCTGAGAAC-3′ and reverse: 5′-TGGTGAAGA CGCCAGTGGA-3′.

The CYP1A1 primers were PPH01271E (SABiosciences).

Western blotting analysis

NHEKs were incubated with lysis buffer (Complete Lysis-M, Roche Applied Science, Indianapolis, IN). Lysate protein concentration was measured using BCA Protein Assay kit (Pierce, Rockford, IL). Equal amounts of protein (40 μg) were dissolved in NuPage LDS Sample Buffer (Invitrogen) and 10% NuPage Sample Reducing Agent (Invitrogen). Lysates were boiled at 70 °C for 10 minutes and loaded and run on 4–12% NuPage Bis-Tris Gels (Invitrogen) at 200 V for 40 minutes. The proteins were transferred onto polyvinylidene fluoride membranes (Invitrogen) and blocked in 2% BSA in 0.1% Tween-20 (Sigma-Aldrich) and Tris-buffered saline. Membranes were probed with anti-AhR, anti-CYP1A1, anti-Nrf2, anti-AhRR, or anti-Nqo1 antibodies overnight at 4 °C. The secondary antibody used was anti-rabbit or anti-mouse horseradish peroxidase-conjugated IgG antibody. Protein bands were detected using the Western Breeze kit (Invitrogen). Densitometric analysis of protein band was performed using ImageJ software (NIH).

Detection of ROS production

DCFH-DA (Molecular Probes) is a cell-permeable non-fluorescent probe that is de-esterified intracellularly and oxidized to highly fluorescent 2′,7′-dichlorofluorescein in the presence of ROS. NHEKs were incubated with DCFH-DA (5 μM) for 30 minutes at 37 °C, and the fluorescence signal of 2′,7′-dichlorofluorescein (Ex = 490 nm), the oxidation product of DCFH-DA, was analyzed using a D-Eclipse confocal laser scanning microscope (Nikon).

ELISA

An IL-8 ELISA kit (Invitrogen) and a highly sensitive 8-OHdG ELISA kit (Japan Institute for the Control of Aging, Shizuoka, Japan)

were used according to the manufacturer's protocol. Nuclear proteins from NHEKs were extracted using NE-PER Nuclear and Cytoplasmic Extraction Reagents (Thermo Scientific, Rockford, IL). Optical density was measured using Labsystems Multiskan MS Analyzer (Thermo Bionalysis Japan, Tokyo, Japan).

ELISA-based Nrf2 transcriptional assay

Protein levels of Nrf2 interacted with an oligonucleotide contained in ARE were measured by TransAM Nrf2 (Active Motif, Carlsbad, CA). After KCZ treatment for 12 hours, nuclear extracts (10 μg) from NHEKs were used as samples. Optical density was measured using Labsystems Multiskan MS Analyzer (Thermo Bionalysis Japan).

Transfection with AhR, Nrf2, or AhRR-targeted specific small interference RNA

SiRNA targeted against AhR (si-AhR, s1200), Nrf2 (si-Nrf2, s9492) and AhRR (si-AhRR, s22144) and siRNA consisting of a scrambled sequence that would not lead to specific degradation of any cellular message (si-control) were purchased from Ambion (Austin, TX). NHEKs cultured in 24-well plates were incubated with mix from HiPerFect Transfection kit (Qiagen, Courtaboeuf, France) containing 10 nM siRNA and 3.0 μl of HiPerFect reagent in 0.5 ml of culture medium. After a 48-hour incubation period, siRNA-transfected NHEKs were treated with KCZ for 48 hours. siRNA transfection showed no effect on cell viability, as demonstrated by microscopic examination (data not shown).

Statistical analysis

Unpaired Student's *t*-test was used to analyze results, and a *P*-value <0.05 was considered to indicate a statistically significant difference.

CONFLICT OF INTEREST

The authors state no conflict of interest.

ACKNOWLEDGMENTS

This study was supported by a grant from the Ministry of Health, Labour, and Welfare, Japan, and the Environmental Technology Development Fund of the Ministry of the Environment, Japan.

SUPPLEMENTARY MATERIAL

Supplementary material is linked to the online version of the paper at http://www.nature.com/jid

REFERENCES

Adhami VM, Afaq F, Ahmad N (2003) Suppression of ultraviolet B exposure-mediated activation of NF-kappaB in normal human keratinocytes by resveratrol. *Neoplasia* 5:74–82

Akintobi AM, Villano CM, White LA (2007) 2,3,7,8-Tetrachlorodibenzo-p-dioxin (TCDD) exposure of normal human dermal fibroblasts results in AhR-dependent and -independent changes in gene expression. *Toxicol Appl Pharmacol* 220:9–17

Bäck O, Scheynius A, Johansson SG (1995) Ketoconazole in atopic dermatitis: therapeutic response is correlated with decrease in serum IgE. *Arch Dermatol Res* 287:448–51

Baggiolini M, Clark-Lewis I (1992) Interleukin-8, a chemotactic and inflammatory cytokine. *FEBS Lett* 307:97–101

Bickers DR, Athar M (2006) Oxidative stress in the pathogenesis of skin disease. *J Invest Dermatol* 126:2565–75

Bos JD, Meinardi MM (2000) The 500 Dalton rule for the skin penetration of chemical compounds and drugs. *Exp Dermatol* 9:165–9

Casley WL, Ogrodowczyk C, Larocque L *et al.* (2007) Cytotoxic doses of ketoconazole affect expression of a subset of hepatic genes. *J Toxicol Environ Health A* 70:1946–55

Casper RF, Quesne M, Rogers IM *et al.* (1999) Resveratrol has antagonist activity on the aryl hydrocarbon receptor: implications for prevention of dioxin toxicity. *Mol Pharmacol* 56:784–90

Chin TW, Loeb M, Fong IW (1995) Effects of an acidic beverage (Coca-Cola) on absorption of ketoconazole. *Antimicrob Agents Chemother* 39:1671–5

Darabi K, Hostetler SG, Bechtel MA *et al.* (2009) The role of Malassezia in atopic dermatitis affecting the head and neck of adults. *J Am Acad Dermatol* 60:125–36

De Pedrini P, Rapisarda R, Spanò G (1988) The effect of ketoconazole on sebum secretion in patients suffering from acne and seborrhea. *Int J Tissue React* 10:111–3

Farr PM, Krause LB, Marks JM *et al.* (1985) Response of scalp psoriasis to oral ketoconazole. *Lancet* 2:921–2

Fritsche E, Schäfer C, Calles C *et al.* (2007) Lightening up the UV response by identification of the aryl hydrocarbon receptor as a cytoplasmatic target for ultraviolet B radiation. *Proc Natl Acad Sci USA* 104:8851–6

Gupta AK, Nicol K, Batra R (2004) Role of antifungal agents in the treatment of seborrheic dermatitis. *Am J Clin Dermatol* 5:417–22

Haarmann-Stemmann T, Bothe H, Abel J (2009) Growth factors, cytokines and their receptors as downstream targets of aryl hydrocarbon receptor (AhR) signaling pathways. *Biochem Pharmacol* 77:508–20

Henry EC, Gasiewicz TA (2008) Molecular determinants of species-specific agonist and antagonist activity of a substituted flavone towards the aryl hydrocarbon receptor. *Arch Biochem Biophys* 472:77–88

Hwang YP, Choi JH, Yun HJ *et al.* (2011) Anthocyanins from purple sweet potato attenuate dimethylnitrosamine-induced liver injury in rats by inducing Nrf2-mediated antioxidant enzymes and reducing COX-2 and iNOS expression. *Food Chem Toxicol* 49:93–9

Imamura T, Kanagawa Y, Matsumoto S *et al.* (2007) Relationship between clinical features and blood levels of pentachlorodibenzofuran in patients with Yusho. *Environ Toxicol* 22:124–31

Jaiswal AK (2004) Nrf2 signaling in coordinated activation of antioxidant gene expression. *Free Radic Biol Med* 36:1199–207

Khan IU, Bickers DR, Haqqi TM *et al.* (1992) Induction of CYP1A1 mRNA in rat epidermis and cultured human epidermal keratinocytes by benz(a) anthracene and beta-naphthoflavone. *Drug Metab Dispos* 20:620–4

Kanda N, Watanabe S (2006) Suppressive effects of antimycotics on tumor necrosis factor-alpha-induced CCL27, CCL2, and CCL5 production in human keratinocytes. *Biochem Pharmacol* 72:463–73

Köhle C, Bock KW (2007) Coordinate regulation of phase I and II xenobiotic metabolisms by the Ah receptor and Nrf2. *Biochem Pharmacol* 73:1853–62

Korashy HM, Shayeganpour A, Brocks DR *et al.* (2007) Induction of cytochrome P450 1A1 by ketoconazole and itraconazole but not fluconazole in murine and human hepatoma cell lines. *Toxicol Sci* 97:32–43

Li W, Khor TO, Xu C *et al.* (2008) Activation of Nrf2-antioxidant signaling attenuates NFkappaB-inflammatory response and elicits apoptosis. *Biochem Pharmacol* 76:1485–9

Liu Y, Chan F, Sun H *et al.* (2011) Resveratrol protects human keratinocytes HaCaT cells from UVA-induced oxidative stress damage by down-regulating Keap1 expression. *Eur J Pharmacol* 10:130–7

Ma Q, Lu AY (2003) Origins of individual variability in P4501A induction. *Chem Res Toxicol* 16:249–60

Marrot L, Jones C, Perez P *et al.* (2008) The significance of Nrf2 pathway in (photo)-oxidative stress response in melanocytes and keratinocytes of the human epidermis. *Pigment Cell Melanoma Res* 21:79–88

Miao W, Hu L, Scrivens PJ *et al.* (2005) Transcriptional regulation of NF-E2 p45-related factor (NRF2) expression by the aryl hydrocarbon receptor-xenobiotic response element signaling pathway: direct cross-talk between phase I and II drug-metabolizing enzymes. *J Biol Chem* 280: 20340–8

Mimura J, Ema M, Sogawa K *et al.* (1999) Identification of a novel mechanism of regulation of Ah (dioxin) receptor function. *Genes Dev* 13:20–5

Nakashima T, Sato E, Niwano Y *et al.* (2007) Inhibitory or scavenging action of ketoconazole and ciclopiroxolamine against reactive oxygen species released by primed inflammatory cells. *Br J Dermatol* 156:720–7

Nandal S, Dhir A, Kuhad A *et al.* (2009) Curcumin potentiates the anti-inflammatory activity of cyclooxygenase inhibitors in the cotton pellet granuloma pouch model. *Methods Find Exp Clin Pharmacol* 31:89–93

Natarajan VT, Singh A, Kumar AA *et al.* (2010) Transcriptional upregulation of Nrf2-dependent phase II detoxification genes in the involved epidermis of vitiligo vulgaris. *J Invest Dermatol* 130:2781–9

Rinaldi AL, Morse MA, Fields HW *et al.* (2002) Curcumin activates the aryl hydrocarbon receptor yet significantly inhibits (−)-benzo(a)pyrene-7R-trans-7,8-dihydrodiol bioactivation in oral squamous cell carcinoma cells and oral mucosa. *Cancer Res* 62:5451–6

Saladi R, Austin L, Gao D *et al.* (2003) The combination of benzo[a]pyrene and ultraviolet A causes an *in vivo* time-related accumulation of DNA damage in mouse skin. *Photochem Photobiol* 77:413–9

Tsuchiya Y, Nakajima M, Itoh S *et al.* (2003) Expression of aryl hydrocarbon receptor repressor in normal human tissues and inducibility by polycyclic aromatic hydrocarbons in human tumor-derived cell lines. *Toxicol Sci* 72:253–9

Tsuji G, Takahara M, Uchi H *et al.* (2011) An environmental contaminant, benzo(a)pyrene, induces oxidative stress-mediated interleukin-8 production in human keratinocytes via the aryl hydrocarbon receptor signaling pathway. *J Dermatol Sci* 62:42–9

Vogel CF, Sciullo E, Li W *et al.* (2007) RelB, a new partner of aryl hydrocarbon receptor-mediated transcription. *Mol Endocrinol* 21:2941–55

Wang SL, Tsai PC, Yang CY *et al.* (2008) Increased risk of diabetes and polychlorinated biphenyls and dioxins: a 24-year follow-up study of the Yucheng cohort. *Diabetes Care* 31:1574–9

Yeager RL, Reisman SA, Aleksunes LM *et al.* (2009) Introducing the ''TCDD-inducible AhR-Nrf2 gene battery''. *Toxicol Sci* 111:238–46

Young CN, Koepke JI, Terlecky LJ *et al.* (2008) Reactive oxygen species in tumor necrosis factor-alpha-activated primary human keratinocytes: implications for psoriasis and inflammatory skin disease. *J Invest Dermatol* 128:2606–14